AD-A092 603 TENNESSEE UNIV KNOXVILLE ULTRASONICS LAB F/6 20/1
RAYLEIGH REFLECTIONS AND NONLINEAR ACOUSTICS OF SOLIDS.(U)
OCT 80 M A BREAZEALE N00014-76-C-0177
UNCLASSIFIED TR-18 NL

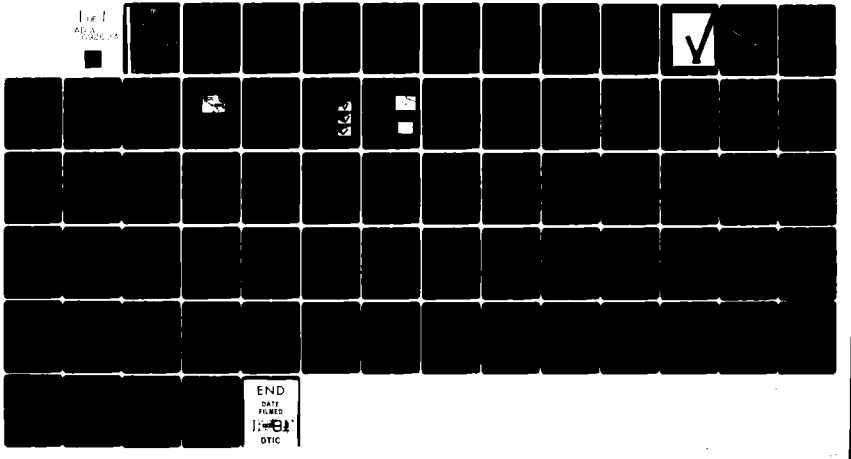

END
DATE FILMED
1-81
DTIC

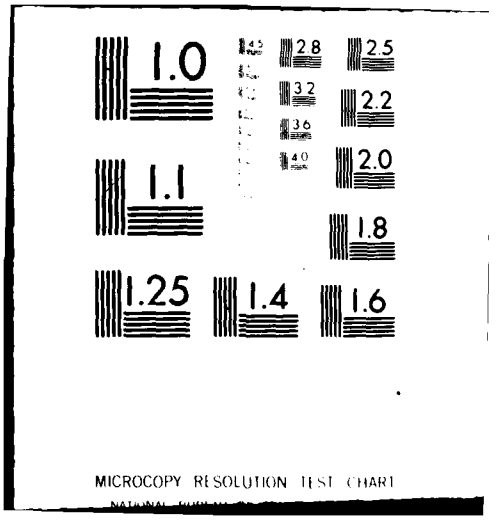
1.0
2.8
2.5
3.2
2.2
3.6
4.0
2.0
1.1
1.8
1.25
1.4
1.6
MICROCOPY RESOLUTION TEST CHART

LEVEL II

OFFICE OF NAVAL RESEARCH
CONTRACT NO. N00014-76-C-0177
PROJECT NO. 384-306

TECHNICAL REPORT NO. 18

RAYLEIGH REFLECTIONS AND NONLINEAR ACOUSTICS OF SOLIDS

M.A. BREAZEALE
PRINCIPAL INVESTIGATOR

ULTRASONICS LABORATORY
DEPARTMENT OF PHYSICS

THE UNIVERSITY OF TENNESSEE
Knoxville, Tennessee

OCTOBER 1980

Unclassified

SECURITY CLASSIFICATION OF THIS PAGE (When Data Entered)

REPORT DOCUMENTATION PAGE	READ INSTRUCTIONS BEFORE COMPLETING FORM
1. REPORT NUMBER: 14 - 18	2. GOVT ACCESSION NO.: AD-A092 603
3. RECIPIENT'S CATALOG NUMBER:	
4. TITLE (and Subtitle): RAYLEIGH REFLECTIONS AND NONLINEAR ACOUSTICS OF SOLIDS.	5. TYPE OF REPORT & PERIOD COVERED: Interim
	6. PERFORMING ORG. REPORT NUMBER:
7. AUTHOR(s): M. A. Breazeale	8. CONTRACT OR GRANT NUMBER(s): N00014-76-C-0177
9. PERFORMING ORGANIZATION NAME AND ADDRESS: Dept. of Physics, The University of Tennessee, Knoxville, TN 37916	10. PROGRAM ELEMENT, PROJECT, TASK AREA & WORK UNIT NUMBERS: 1.194
11. CONTROLLING OFFICE NAME AND ADDRESS: Office of Naval Research, Code 421, Department of the Navy, Arlington, VA 22217	12. REPORT DATE: October 1980
	13. NUMBER OF PAGES: 65
14. MONITORING AGENCY NAME & ADDRESS(if different from Controlling Office)	15. SECURITY CLASS. (of this report): Unclassified
	15a. DECLASSIFICATION/DOWNGRADING SCHEDULE

16. DISTRIBUTION STATEMENT (of this Report)

Approved for public release; distribution unlimited.

17. DISTRIBUTION STATEMENT (of the abstract entered in Block 20, if different from Report)

18. SUPPLEMENTARY NOTES

19. KEY WORDS (Continue on reverse side if necessary and identify by block number)

Ultrasonic goniometer
Ultrasonic wave reflection
Rayleigh angle
Liquid-solid layer-solid interface
Leaky surface waves

(continued on reverse side)

20. ABSTRACT (Continue on reverse side if necessary and identify by block number)

Technical Report No. 18 is a summary of recent research on two topics: Part I. Schlieren Studies of Ultrasonic Waves, and Part II. Nonlinear Acoustics of Solids.

Part I. The report begins with the description of a unique goniometer for use in a schlieren system for visualization of ultrasonic waves in liquids. By using the properties of parallelograms we were able to produce a precision goniometer without use of precision machine shop facilities. The

DD FORM 1 JAN 73 1473 EDITION OF 1 NOV 65 IS OBSOLETE

S/N 0102-LF-014-6601

A

SECURITY CLASSIFICATION OF THIS PAGE (When Data Entered)

19 (continued)

Nonlinear acoustics of solids
Nonlinearity parameters
Third-order elastic constants
Harmonic generation
Quantum mechanical theory of nonlinear interactions

20 (continued)

goniometer is used to obtain schlieren photographs of leaky Rayleigh waves excited on an Al_2O_3 layer on a stainless steel reflector immersed in water, showing that the Rayleigh wave velocity in this case is less than that of either a water-Al_2O_3 layer or a water-stainless steel layer.

Part II. Four subjects are covered: (1) The Nonlinearity Parameters and Third-Order Elastic Constants of Copper between 300 and 3 K; (2) Measurement of Nonlinearity Parameters in Small Solid Samples by the Harmonic Generation Technique; (3) Relationship between Solid Nonlinearity Parameters and Thermodynamic Grüneisen Parameters; (4) Quantum Mechanical Theory of Nonlinear Interaction of Ultrasonic Waves.

OFFICE OF NAVAL RESEARCH
CONTRACT NO. N00014-76-C-0177
PROJECT NO. 384-306

RAYLEIGH REFLECTIONS AND NONLINEAR ACOUSTICS OF SOLIDS

by

M. A. Breazeale

TECHNICAL REPORT NO. 18

Ultrasonics Laboratory
Department of Physics
The University of Tennessee 37916

October 1980

INTRODUCTION

In Technical Report Nos. 15, "Ultrasonic Wave Reflection at Liquid-Solid Interfaces," and 17, "Studies of Linear and Nonlinear Ultrasonic Phenomena," we presented summaries of our contributions to certain subjects. Technical Report No. 18 is intended to expand on the summary and bring it up to date. It is divided into two parts.

Part I. Schlieren Studies of Ultrasonic Waves

The Report begins with the description of a unique goniometer designed by members of the Ultrasonic Group for use in the schlieren system for visualization of ultrasonic waves in liquids. By using the properties of parallelograms we were able to produce a precision goniometer without use of precision machine shop facilities. The second paper presents some photographs made with the goniometer in the schlieren system and shows the effect of a layer of Al_2O_3 on a stainless steel reflector of ultrasonic waves in water. The leaky Rayleigh wave excited in the Al_2O_3 layer has a velocity smaller than that exicted either at a water-stainless steel interface or at a water-Al_2O_3 interface.

Part II. Nonlinear Acoustics of Solids

In relatively large single crystal samples (1 inch in diameter and 1 inch long) one can measure such things as "The Nonlinearity Parameters and Third-Order Elastic Constants of Copper between 300 and 3° K" as reported in Paper No. 3. The fact that the measurements can be made to low temperatures is especially important, as the effect of thermal motion of the atoms is ignored in many theories. This means that they are strictly applicable only at 0° K. For comparison with these theories, then, we measure to the lowest readily obtainable temperature.

A problem encountered in the study of the nonlinear properties of solids is the fact that oftentimes it is difficult to grow large single crystals of interesting substances. Ordinarily we use a 30 MHz ultrasonic wave of finite amplitude to determine the nonlinearity parameters of single crystals 1 inch in diameter and 1 inch long. The amplitude of the second harmonic, which must be measured absolutely, typically is of the order of 10^{-2} Å in these samples. We posed for ourselves a question: Given our desire to measure nonlinearity parameters, what is the smallest sample one can measure with present technique? The fourth paper, "Measurement of Nonlinearity Parameters in Small Solid Samples by the Harmonic Generation Technique," is an attempt to answer the question.

Another question of fundamental importance to nonlinear acoustics of solids is the relationship between the nonlinearity parameter measured acoustically and the Grüneisen parameter which comes from measurement of thermal properties. This question is given a relatively simple, and almost complete, answer in the fifth paper on "Relationship between Solid Nonlinearity Parameters and Thermodynamic Grüneisen Parameters." This paper was based on the oral presentation given at the joint meeting of the Acoustical Society of America and the Acoustical Society of Japan. This was an especially appropriate audience since two of the authors were from the United States and one was from Japan.

The final paper in this Report, "Quantum Mechanical Theory of Nonlinear Interaction of Ultrasonic Waves," answers in part another fundamental question of nonlinear acoustics. Presumably in the correspondence limit the quantum mechanical description of phonon-phonon interaction would become identical to the description (based on nonlinear

elasticity)of the scattering of one acoustical disturbance by another. But this assumption was hard to prove. The paper provides specific examples. It begins with the general quantum mechanical description of phonon-phonon interaction and specializes the description to that of two collinear phonons of frequency ν which interact to produce a phonon of frequency 2ν. (This comes from energy conservation: $h\nu + h\nu = 2h\nu$.) By maintaining the wave description (avoiding quantization), one is able to show that the mathematical result is identical to that previously obtained from a generalization of elasticity. This is true also in the description of third harmonic generation. In third harmonic generation one is able to show, in addition, that the small term in the third harmonic amplitude which contains fourth-order elastic constants in fact comes from four-phonon interactions in the quantum mechanical picture, whereas all of the other terms (those involving second-order and third-order elastic constants) resulted from three-phonon interactions. The advantage of the quantum mechanical approach lies primarily in the fact that the path from the general description to the particular application is explicitly marked, and the point at which one makes any particular simplifying assumption can be located unambiguously.

PART I. SCHLIEREN STUDIES OF ULTRASONIC WAVES

PART II. NONLINEAR ACOUSTICS OF SOLIDS

A UNIQUE GONIOMETER FOR USE IN SCHLIEREN VISUALIZATION OF ULTRASONIC WAVES

M. A. Breazeale
Department of Physics
The University of Tennessee
Knoxville, Tennessee 37916

Introduction

Alignment problems encountered in the use of schlieren systems have been recognized, and often solved, by a number of investigators. For example, Fig. 1 is a schlieren photograph[1] of the interaction between an ultrasonic beam of Gaussian cross section[2] and a leaky wave at an interface. The fact that the reflected beam is displaced to the left, rather than to the right, results from a fine periodic structure (grating) at the interface. The periodic structure shifts the phase of a leaky wave trapped at the interface by 180°, and causes the energy flow to follow the path indicated in Fig. 2.

The photograph of Fig. 1 was made only after expenditure of considerable effort. The grating periodicity of 0.178 mm required not only precision alignment, but also the maintenance of the precision alignment as the incident angle was changed. Subsequently a movie was made[3] to show in detail what happens as the incident angle is changed. For the movie the point of contact between the ultrasonic beam and the reflecting interface had to remain the same for all incident angles. This required a precision goniometer capable of rotating the transducer along a circular path centered at the point of contact between the ultrasonic beam and the reflecting interface.

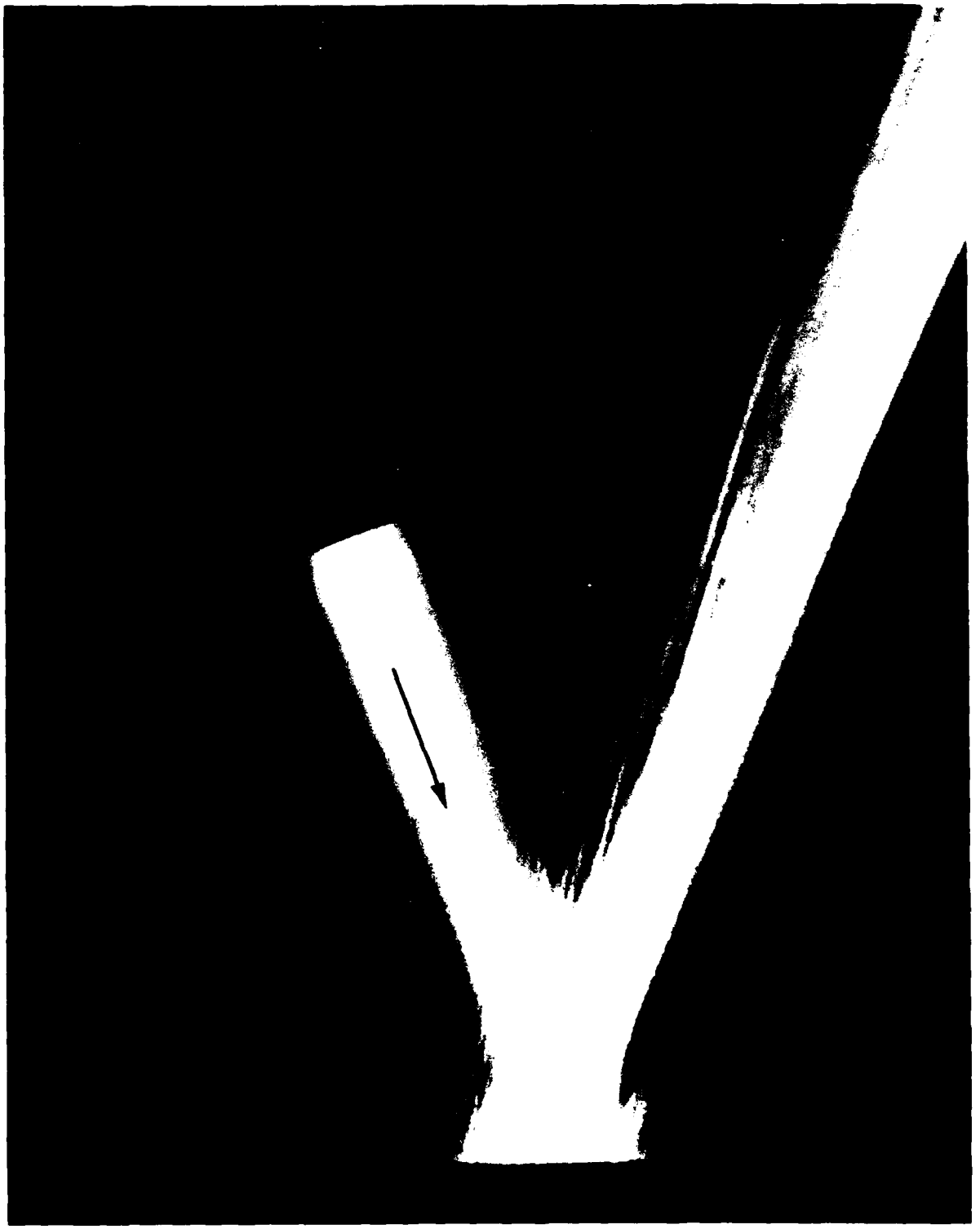

Figure 1. Schlieren photograph of an ultrasonic beam of Gaussian cross section reflected from a brass grating in water.

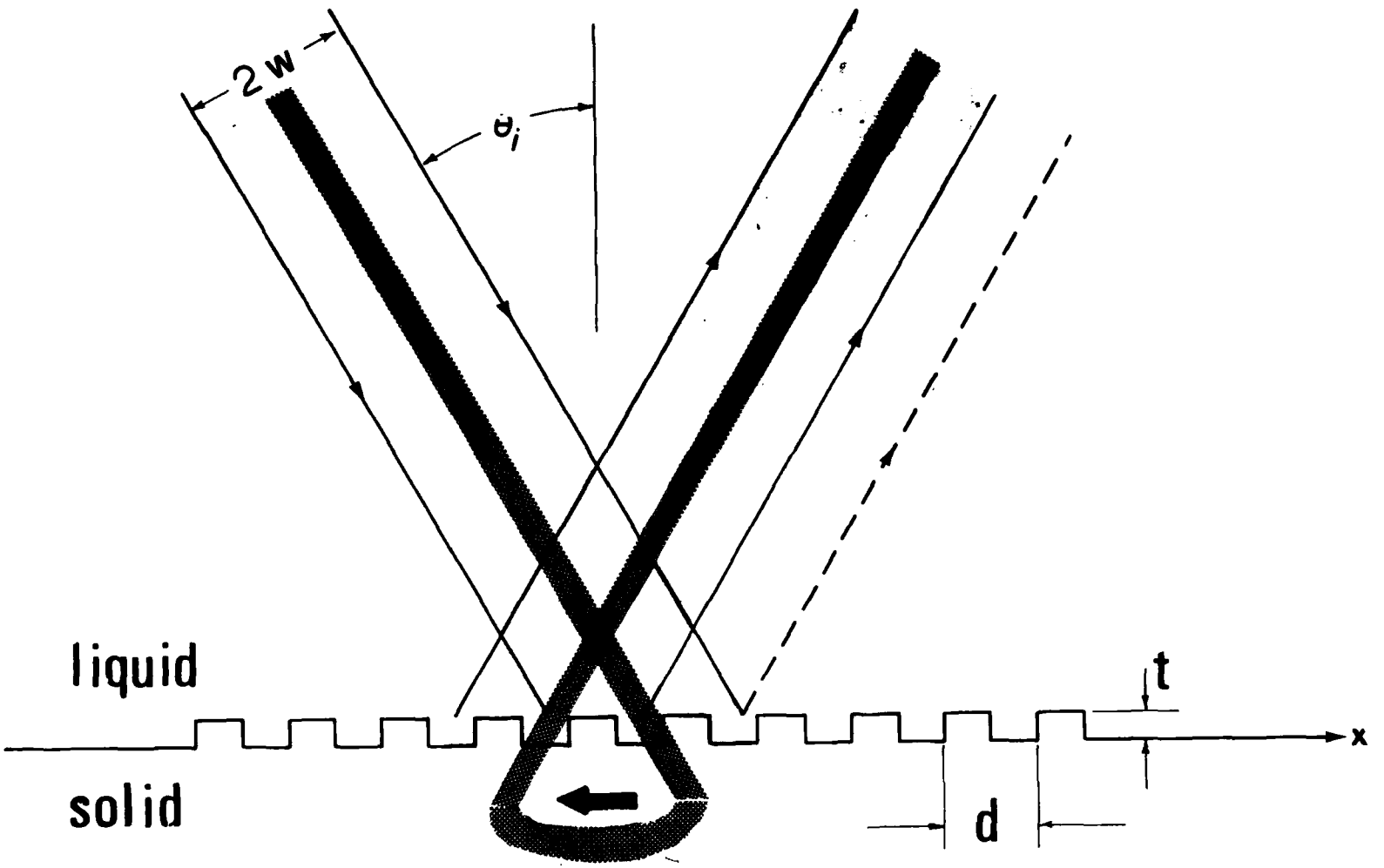

Figure 2. Direction of energy flow in ultrasonic beam shown in Figure 1.

The purpose of the present discussion is not to give an exhaustive description of the phenomena that occur when an ultrasonic beam is reflected at a liquid-solid interface. Rather, the purpose of the present discussion is to describe a precision goniometer that has made an experimental study of such phenomena possible.

Description of Goniometer

The design of the goniometer can be understood by observing geometrical properties of parallelograms. Suppose a parallelogram were constructed by placing bearings at the four corners. The parallelogram then could distort as shown in Fig. 3, in which two positions are drawn. The property of interest here is the fact that any point on the top edge of the parallelogram traces out a circle centered at a corresponding point on the bottom edge. This is true not only at the corner, labelled A_1 and A_2, but also for any other point (e.g., B_1 and B_2), as indicated. The centers of the circles are C_A and C_B, respectively.

Let us now remove the bottom edge of the parallelogram, but fix the position of the bearings by adding an auxiliary support. Further, let us form another parallelogram by adding a horizontal piece, as indicated in Fig. 4. To the two horizontal portions of the new parallelogram, let us now add a new set of bearings and attach a new vertical member. A transducer attached to this piece has the capability we desire: the possibility to rotate about a point, the point of intersection of the two dotted lines. A reflecting surface placed at the position indicated can be studied in detail. The ultrasonic beam reflected from it will reflect from exactly the same point on the interface for all incident angles.

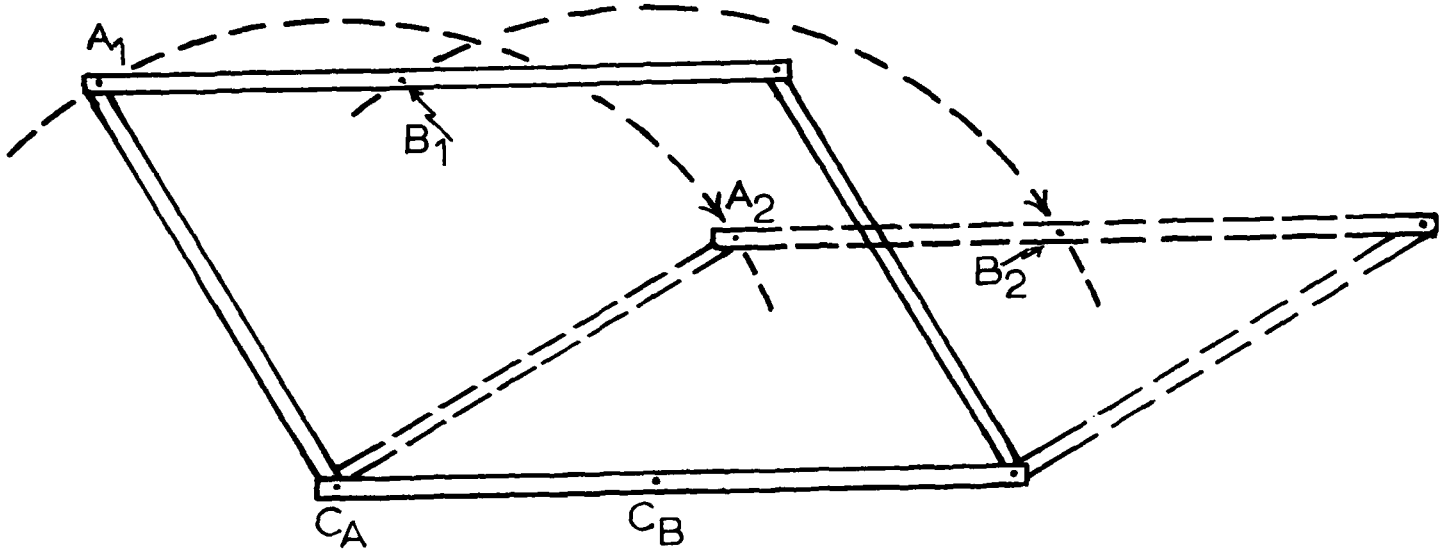

Figure 3. A parallelogram with bearings at corners distorts as indicated. As the point A_1 follows a circular path to arrive at A_2, the point B_1 also follows a circular path to arrive at B_2. The centers of curvature are C_A and C_B, respectively.

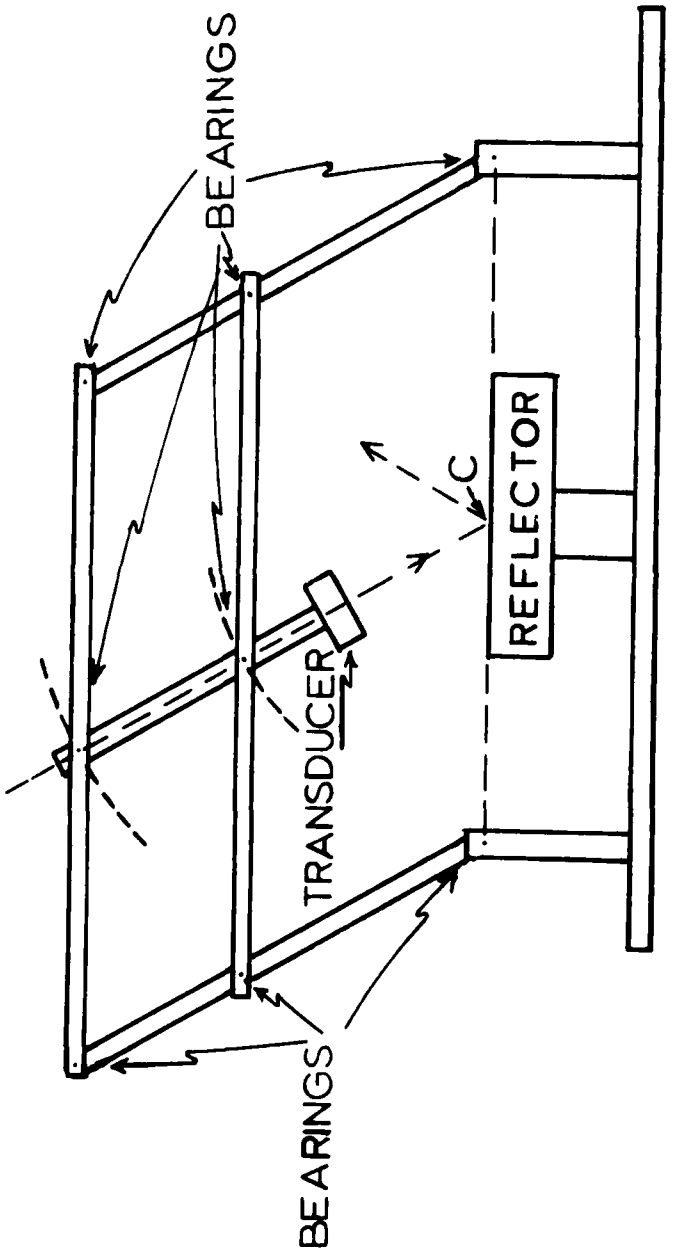

Figure 4. Goniometer constructed on the principles outlined in Fig. 3. The transducer remains aimed at C, the center of curvature, as the incident angle is changed through distortion of the parallelogram.

A goniometer using the principles described has been in use in the Ultrasonics Laboratory at The University of Tennessee for several years. A photograph of the goniometer and one lens of the schlieren system is shown in Fig. 5. In the photograph several refinements are observable:

1. The support for the transducer has a dog-leg in it. This avoids problems that would arise for incident angles great enough that the edge of the water tank would interfere with transducer motion.
2. A scale is provided on one of the supports so the incident angle can be measured directly.
3. A worm gear is used to make precision adjustment of the incident angle.
4. The entire system is counterbalanced by lead bricks.

Finally, it is obvious that the same effect could be accomplished by use of a circular track of sufficiently large diameter. Such systems have been constructed in other laboratories, but they require complicated and expensive machine shop work. The advantages of the parallelogram goniometer are:

1. Simplicity of construction. (One only needs to bore the holes for the bearings at the correct positions. No large or complicated machine shop facilities are needed.)
2. Precise adjustment possible (no stick-slip in the movement).
3. Maintenance of precision over long periods.

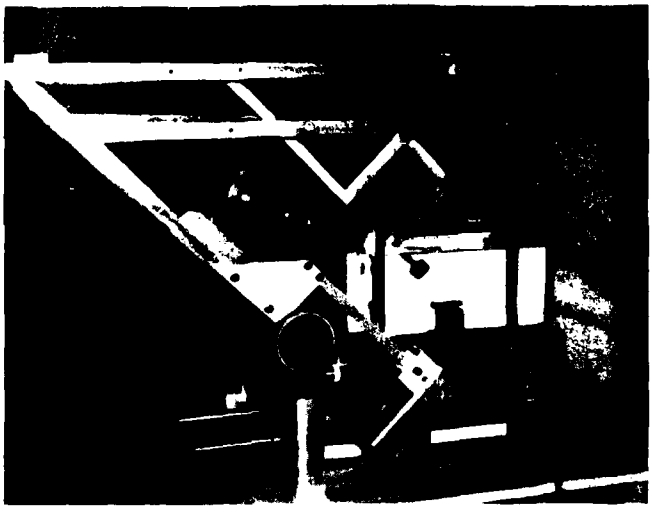

Figure 5. Parallelogram ultrasonic goniometer in a schlieren system.

Conclusion

This new approach to an old problem has produced a goniometer that is working effectively in a schlieren system having an aperture of 8 inches. The principle on which the goniometer is based can be used with even larger systems without a fundamental increase in the complication of construction.

References

1. M. A. Breazeale and Michael A. Torbett, "Backward Displacement of Waves Reflected from an Interface Having Superimposed Periodicity," Appl. Phys. Lett. 29, 456-58 (1976).

2. Franklin D. Martin and M. A. Breazeale, "A Simple Way to Eliminate Diffraction Lobes Emitted by Ultrasonic Transducers," J. Acoust. Soc. Am. 49, 1668-69 (1971).

3. M. A. Breazeale, "Wave Interactions at Plane and Grating Interfaces," J. Acoust. Soc. Am. 60, Suppl. No. 1, S53 (1976).

LEAKY WAVE GENERATION AT Al_2O_3 LAYER ON STAINLESS STEEL IN WATER

Laszlo Adler and Daniel L. Butler

Department of Physics
The University of Tennessee
Knoxville, Tennessee 37916

Abstract

When a finite ultrasonic beam with a Gaussian amplitude distribution is reflected from an Al_2O_3 layer on stainless steel in water the reflected amplitude field distribution indicates leaky wave generation. The angle at which the leaky wave is generated defines the leaky wave velocity. The leaky wave velocity of this structure is measured as a function of kh (where k is the wave number and h is the layer thickness). The effect of the presence of the layer on the reflected amplitude distribution is discussed.

1. Introduction and Background

The reflection of ultrasonic waves at a liquid-solid interface as a function of incident angle is a basic boundary value problem. For infinite plane waves one solves the wave equation with appropriate B.C. Recently interest has been focused on the physically realistic problem of the reflection of a finite beam of some well-defined shape from the liquid-solid interface. Both experimental[1,2] and theoretical[3] analysis have established the existence of the so-called leaky Rayleigh waves at the liquid-solid boundary. The existence of these waves is easily demonstrated by a Schlieren picture of an incident Gaussian ultrasonic beam reflected below, at and above the Rayleigh angle. Figure 1 shows the case for water-stainless steel interface. The middle picture is taken at the Rayleigh angle about 30.5°. The angle of incidence is such that the refracted wave is coupled along the interface and leaks back to the liquid as it propagates. This leaky wave together with the specularly reflected field produces the total reflected field.

The theoretical analysis of this finite beam problem was carried out by Bertoni and Tamir.[3] In their development of an analytical approximation to the reflection integral, Bertoni and Tamir show that it divides into two parts and can be written as

$$v_{refl}(x,z) = v_0(x,z) + v_1(x,z) . \qquad (1)$$

$v_0(x,z)$ represents a specular reflection, which resembles the incident beam in its amplitude distribution but is shifted 180° in phase. $v_1(x,z)$ is the surface component, which is in phase with the incident beam over part of the interface and out of phase over the remainder; its amplitude distribution is, in general, significantly different from that of the incident beam and the specular component.

(a)

(b)

(c)

Figure 1 - Reflection of a Gaussian Ultrasonic Beam from a Water-Stainless Steel Surface for Incident Angles (a) 25°, (b) 30.5° (Rayleigh Angle), (c) 40°.

1979 Ultrasonics Symposium Proceedings, IEEE Cat. #79CH1492-9SU

For a Gaussian incident beam, as used in the experiments described below, Bertoni and Tamir[3] obtained an analytical approximation valid at the interface. In order to compare theory with experiment, Breazeale, Adler, and Scott[2] corrected the approximation for points in the liquid halfspace. The expressions for the leaky wave field components are:

$$V_0(x_r,z_r) =$$

$$\frac{1}{2\pi} \exp \frac{\{-(x_r/w_r)^2+ik[x_r\sin\theta_p+(z_r-z_0)\cos\theta_p]\}}{\sqrt{\pi}w_r\cos\theta_p} \quad (2)$$

$$V_1(x_r,z_r) = -2V_1(x_r,z_r)[1 - \frac{\sqrt{\pi}w_r}{\Delta_s} \exp(\gamma^2)\mathrm{erfc}(\gamma)] \quad (3)$$

where

$$\gamma = \frac{w_r}{\Delta_s} - \frac{x_r}{w_r}, \quad (4)$$

and

$$w^r = w[1 + \frac{2i(z_r-z_0)}{kw^2\cos\theta_p}]^{1/2} . \quad (5)$$

The beam halfwidth w is measured at z_0, θ_p is the liquid-solid equivalent of the Rayleigh angle, and Δ_s is the so-called "Schoch displacement." Δ_s was derived by Schoch in his original lateral displacement theory and was shown to be mathematically equivalent to a surface wave decay constant occurring in the Bertoni-Tamir approximation. It is a complex function of the acoustic velocities and densities of the interface media. The finite beam reflection from the solid layer-solid in water has no theoretical treatment at present. The experimental investigation of this problem will be presented in the next section.

2. Leaky Wave Generation of Solid Layer-Solid Interface in Water

The problem presented here deals with the generation of leaky waves at a liquid-solid layer-solid interface. The problem is shown on Fig. 2.

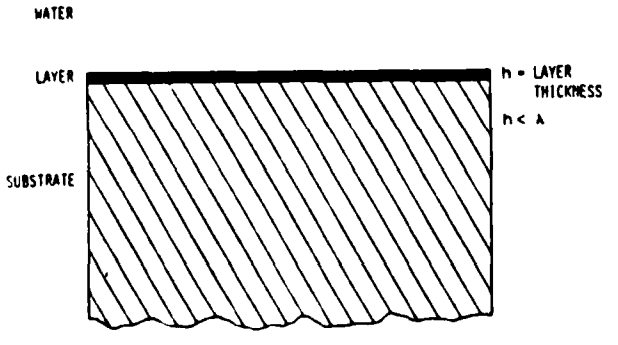

Figure 2 - Water-Solid Layer-Solid Interface.

A solid layer which is of Al_2O_3 ceramic layer is sprayed on a stainless steel block. The reason Al_2O_3 is chosen is because of our previous studies of leaky wave structure on both water-Al_2O_3 and on water-stainless steel.[2] The main part of the experimental arrangement to obtain quantitative data of the reflected beam profile is a specially designed goniometer shown on Fig. 3. A 2-MHz Gaussian transducer sends out some long pulses of 20-30 μsec. The receiver is scanned through about 7 cm, which is the extent of the reflected field.

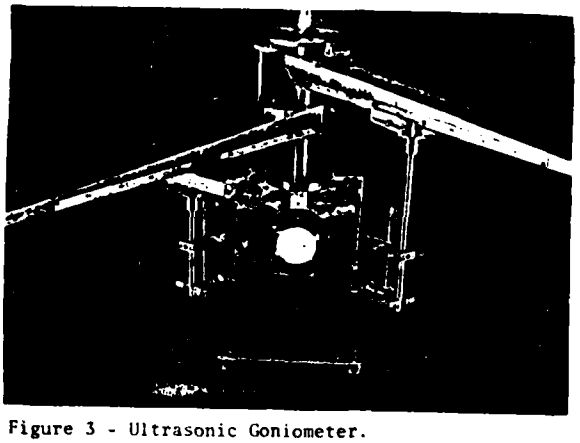

Figure 3 - Ultrasonic Goniometer.

The demonstration of the existence of leaky waves was done in the following ways: The receiver and transducer arms were scanned by small increments of angles until the RF waveforms indicated the phase cancellation. On Fig. 4 the RF waveform reflected from the Al_2O_3-stainless steel in water is shown. The angle at which the phenomena took place is 31.5°. The Rayleigh leaky velocity is calculated to be 2.68×10^5 cm/sec. The thickness of the Al_2O_3 layer is 80μ. The leaky wave velocity from the Al_2O_3 layer-stainless steel was measured as a function of kh. On Fig. 5 the result

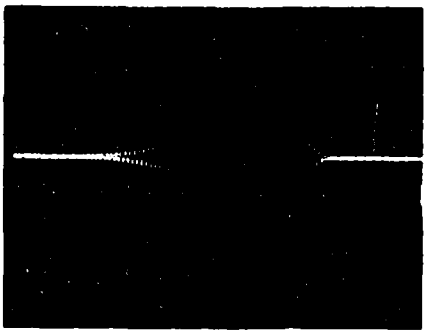

Figure 4 - Received Signal in the Rayleigh Angle Reflection from Water-Al_2O_3 Layer-Stainless Steel.

is plotted. At kh = 0, the Rayleigh leaky velocity of the stainless steel is obtained. As $kh \to \infty$, the Rayleigh velocity of the sprayed Al_2O_3 obtained (in bulk) is 2.18×10^5 cm/sec, which is significantly lower than the velocity of the Al_2O_3 in compact

form (v_R = 5.53 x 10^5 cm/sec). From the asymptotic value of the leaky wave velocity one may obtain the shear velocity and shear modulus as well of the porous material Al_2O_3. Additional knowledge of the wave propagation in the thin layered material may be obtained from the measurements of the amplitude distribution of the reflected wave at the

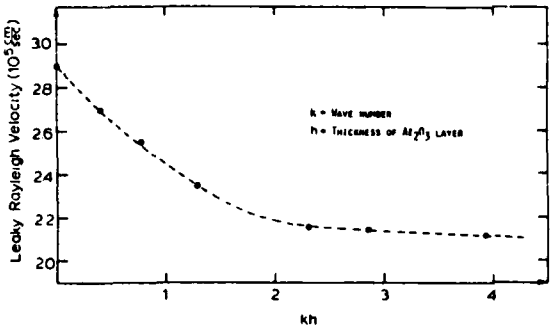

Figure 5 - Variation of Leaky Rayleigh Velocity (V_R) for Water-Al_2O_3 Layer-Stainless Steel Interface.

Rayleigh angle. On Fig. 6 the theoretical values of the reflected field is plotted (solid line). This curve was calculated from the modified Bertoni theory for liquid-steel interface and for the parameters used in the experiment (beam width w = 8 mm, f = 2 MHz, transmitter-interface-receiver total distance z_R = 400 mm). The corresponding experimental points measured are in good agreement with the theory. The effect of the 80μ Al_2O_3 layer on the experimental data is shown by the points. There are several features of these latter data points to consider. First, the amplitude of the first peak is diminished compared to the one without the layer. Second, the null point which indicates the phase cancellation has shifted laterally, indicating that the parameters changed and at phase cancellation between V_0 and V_1 will take place at another point. Since at that point $V_0 = V_1$ equations may be inverted to obtain additional parameters of the interface when a thin layer is present on a substrate. Further theoretical work is required to interpret these experimental findings.

3. Conclusions

The problem of ultrasonic leaky wave propagation in thin (80μ) ceramic layer (Al_2O_3) on stainless steel immersed in water has been investigated. It appears that the leaky wave velocity becomes dispersive with the presence of the layer. The layer also affects the amplitude distribution of the reflected field. No theoretical work is available at present to analyze this problem.

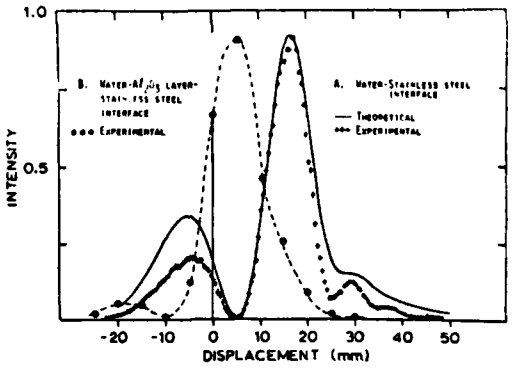

Figure 6 - Amplitude Distribution of a Reflected Gaussian Ultrasonic Beam at the Rayleigh Angle.

4. Acknowledgment

Research supported in part by the Office of Naval Research.

5. References

1. W. G. Neubauer, J. Appl. Phys. 44, 48-55 (1973); W. G. Neubauer and L. R. Dragonette, J. Appl. Phys. 45, 618-622 (1974).

2. M. A. Breazeale, Laszlo Adler, and Gerald W. Scott, J. Appl. Phys. 48, 530-537 (1977).

3. H. L. Bertoni and T. Tamir, Appl. Phys. 2, 157-172 (1973).

PART II. NONLINEAR ACOUSTICS OF SOLIDS

Ultrasonic nonlinearity parameters and third-order elastic constants of copper between 300 °K and 3 °K

W. T. Yost*

John H. Cantrell, Jr.** and

M. A. Breazeale

Department of Physics, The University of Tennessee, Knoxville, TN 37916

ABSTRACT

The ultrasonic harmonic generation technique has been used to extend measurement of the nonlinearity parameters of copper to 3 °K. Comparison of these data and combinations of truly adiabatic TOE constants with predictions of simplified models show that a central force, nearest neighbor model accounts reasonably well for the behavior of copper in the regions of 45 °K and 200 °K and less well at other regions. The central force, nearest neighbor model also gives a good qualitative explanation for the temperature dependence of the combinations of TOE constants that are measured in this investigation.

To be published in the December 1980 issue of Journal of Applied Physics.

I. INTRODUCTION

In the present investigation previously established techniques are used to measure combinations of third-order elastic constants of copper from 300 °K to 3 °K. The technique involves the measurement of the distortion of an ultrasonic wave as it propagates through various copper single crystals.

The development of a capacitive detector and its calibration permit the absolute determination of the amplitudes of finite amplitude ultrasonic waves.[1] Later refinements made possible the extension of these measurements to lower temperatures.[2] These methods have been used to calculate various combinations of TOE constants at low temperatures. Peters, Breazeale, and Paré[3] used this technique to measure combinations of TOE constants of copper to 77 °K. Yost and Breazeale[4] measured combinations of TOE constants of germanium to 77 °K. Bains and Breazeale[5] extended the measurements of germanium to 3 °K. Cantrell and Breazeale[6] measured C_{111} for various samples of fused silica between 300 and 3 °K.

Various investigations of the TOE constants of copper have been made. Daniels and Smith[7] isolated various combinations of TOE constants for copper by measuring the pressure derivatives of second-order elastic constants. Hiki and Granato[8] used pressure derivatives and uniaxial-stress derivatives to determine a complete set of TOE constants for copper at room temperature. Salama and Alers[9] used uniaxial stress derivatives exclusively to determine a complete set of TOE constants for copper at three different temperatures, 295 °K, 77 °K, and 4.2 °K.

Gauster and Breazeale[10] examined combinations of copper TOE constants at room temperature. Peters and Breazeale and Paré[3] extended these measurements to 77 °K. In this paper, we report results of copper which have been measured to 3 °K, by a technique sensitive to changes of TOE constants as a function of temperature. From these measurements, we isolate certain combinations of TOE constants, which are of particular theoretical interest.

The noble metals, of which copper is an example, form face-centered cubic crystal configurations, for which simplified models exist to explain the behavior of TOE constants. For this configuration, we find that if forces of interaction are central in nature, the crystal is free from external stress, and each atom is at a center of inversion,[11] then the Cauchy relations must hold:

Second-order constants $C_{12} = C_{44}$ (1)

Third-order constants $C_{112} = C_{166}$ (2)

and

$$C_{123} = C_{456} = C_{144}$$

Hiki and Granato[8] have shown that if, in addition to the above assumptions, nearest-neighbor repulsive interaction is the predominant contribution to the elastic constants, then the additional relationships also hold.

Second-order constants $C_{11} = 2C_{12} = 2C_{44}$ (3)

Third-order constants $C_{111} = 2C_{112} = 2C_{166}$ (4)

$$C_{123} = C_{456} = C_{144} = 0$$

Our data allow us to make some statements about the validity of the TOE constant Hiki-Granato relations for copper between 3 °K and room temperature.

II. EXPERIMENTAL TECHNIQUE

Pure mode propagation for a longitudinal ultrasonic wave is possible for three principal directions in a cubic crystal. For these directions, the wave equation reduces to[12]

$$\rho_0 \ddot{U} = K_2 \frac{\partial^2 U}{\partial a^2} + (3K_2 + K_3) \frac{\partial U}{\partial a} \frac{\partial^2 U}{\partial a^2} \tag{5}$$

where K_2 and K_3 are combinations of SOE and TOE constants respectively, which are given in Table 1.

Assuming a sinusoidal wave of frequency ω applied at $a = 0$, this equation has the solution

$$U = A_1 \sin(ka - \omega t) - (3K_2 + K_3)/8K_2 A_1^2 k^2 a \cos 2(ka - \omega t) + \ldots \tag{6}$$

where k is the propagation constant $2\pi/\lambda$, a is the propagation distance in the sample, and A_1 is the amplitude of the fundamental. The amplitude A_2 of the second harmonic term is given by

$$A_2 = -[(3K_2 + K_3)/8K_2] A_1^2 k^2 a \, . \tag{7}$$

The measurement of A_2 and A_1 is the basis of the calculation of the nonlinearity parameter β where β is the negative of the ratio of the nonlinear term to the linear term in Eq. (5).

$$\beta = -\left(\frac{3K_2 + K_3}{K_2}\right) . \tag{8}$$

Solving Eq. (7) gives β in terms of measured quantities:

$$\beta = 8 \left(\frac{A_2}{A_1^2} \cdot \frac{1}{k^2 a} \right) . \qquad (9)$$

The quantity K_2 can be determined by the relation $K_2 = \rho v^2$, where v is the velocity of sound in the appropriate direction. For our purposes, we calculated the values of K_2 at the various temperatures from data given in Overton and Gaffney.[13]

III. RESULTS AND DATA ANALYSIS

In these measurements one uses techniques similar to those which have been previously cited in the literature.[3,4,5,6] The room temperature measurements for K_3 in the various crystallographic directions have been taken from Peters, Breazeale, and Paré,[3] since the same samples were used. Figure 1 shows the values of β as a function of temperature in the three principal crystallographic directions. Data from Ref. 3 were used between 300 °K and 77 °K. Those below 77 °K are the new data which were matched to the 77 °K datum from Ref. 3.

Figure 2 shows the values of K_3 as a function of temperature calculated from the data of Fig. 1. The scatter in the K_3 [110] data results in part from the shape of the sample. The [110] faces are at an angle of approximately 15° to the axis of the cylindrical sample. This canting of the sample axis led to difficulties in keeping the sample seated on the ground ring of the capacitive detector.

Error for these measurements are determined by the measurements at room temperature and the relative measurements at the other temperatures. The random errors for K_3 at room temperature are ±1.5%, ±3.2%, and ±2% for values of K_3 in the [100], [110], and [111]

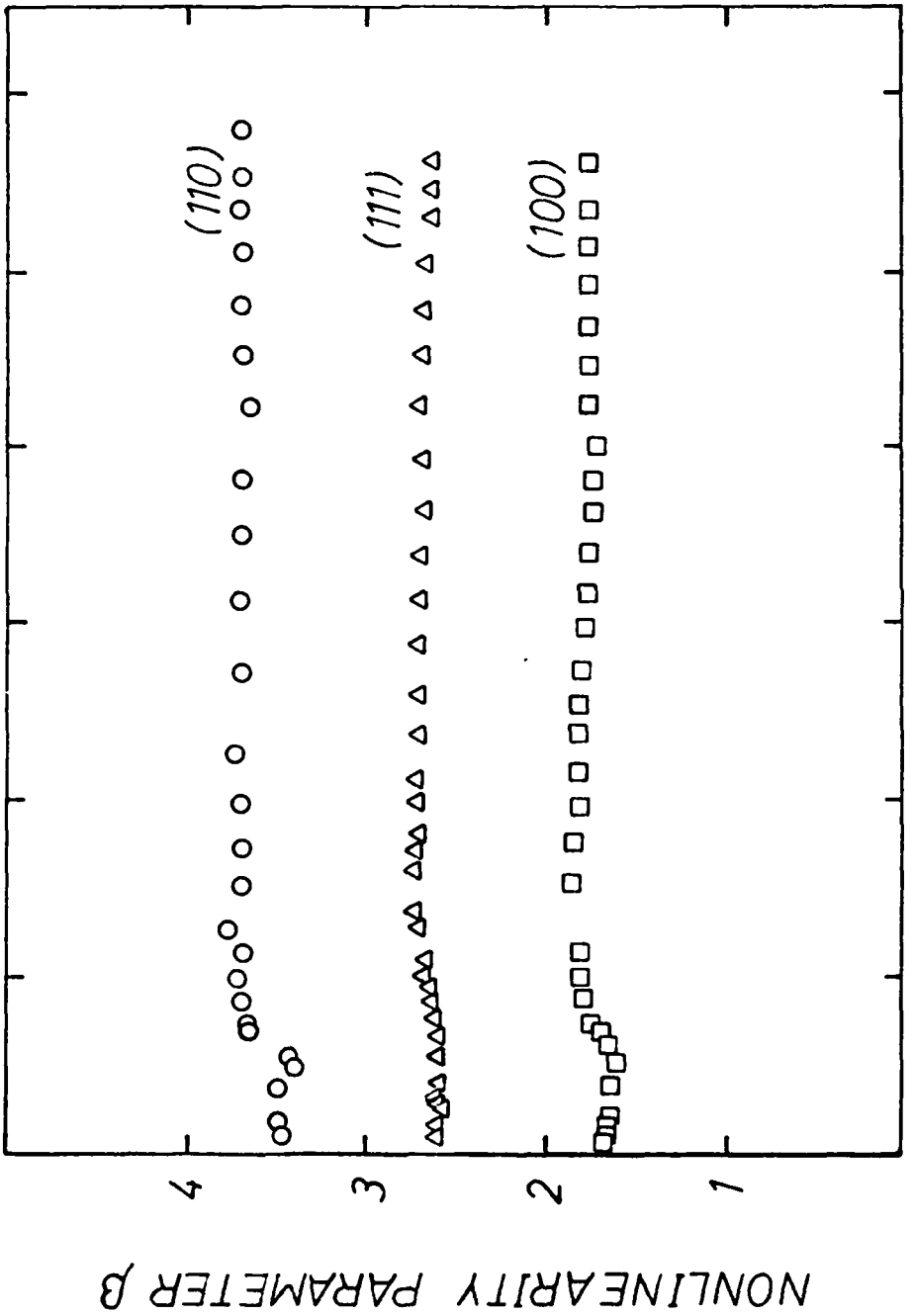

Figure 1. Measured values of the nonlinearity parameter as a function of temperature.

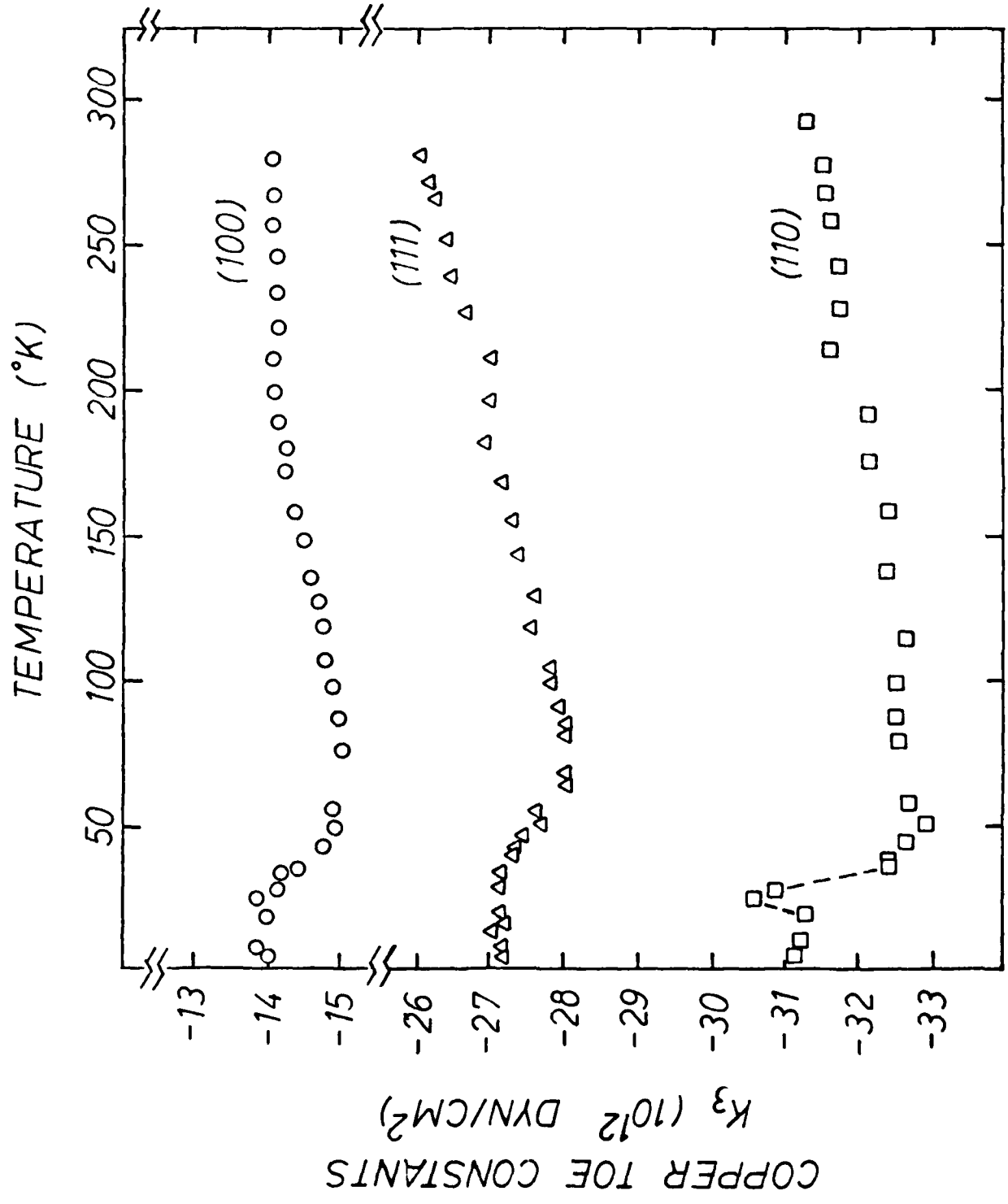

Figure 2. Calculated values of the TOE constant combinations K_3 as a function of temperature.

respectively. Systematic error for these measurements is estimated to be at most ±10%. It is estimated that K_3 can be measured relative to room temperature to well within 3%.

Examination of Table I reveals that the expressions for K_3 are not the simplest combinations of TOE constants available from our data. The K_3 for the [100] direction is the single TOE constant C_{111}. But the K_3 for the other directions also include C_{111}. Thus, it is possible to subtract C_{111} from K_3 for the directions [110] and [111]. Proceeding in this fashion, one is able to obtain the combinations C_{111}, $C_{112} + 4C_{166}$ and $C_{123} + 6C_{144} + 8C_{456}$ plotted in Fig. 3.

IV. DISCUSSION

The nonlinearity parameter β in Fig. 1 is observed to be relatively independent of temperature, as was originally assumed to be the case with the Grüneisen parameter γ.[14,15] As a matter of fact it is possible to make a specialized definition of a "Grüneisen number" which is related to the nonlinearity parameter.[16,17,18] Variation in the value of β does occur between approximately 25 °K and 50 °K, with the most distinct variation occurring in the data for the [110] direction.

When one examines the third-order elastic constants combinations plotted in Fig. 2, the temperature dependence becomes more pronounced. Although the K_3 for [110] direction C_{111} varies by only 8% over the temperature range, and the value of C_{111} at 0 °K is almost identical to the value at 300 °K, the other two orientations exhibit more variation with temperature. Nevertheless, it may be worthwhile to point out that the three curves behave in somewhat the same way. The most obvious temperature variation occurs in the K_3 for the [110] direction. The

Table 1. K_2 and K_3 for [100], [110], and [111] Directions

Direction	K_2	K_3
[100]	C_{11}	C_{111}
[110]	$\frac{C_{11} + C_{12} + 2C_{44}}{2}$	$\frac{C_{111} + 3C_{112} + 12C_{166}}{4}$
[111]	$\frac{C_{11} + 2C_{12} + 4C_{44}}{3}$	$\frac{C_{111} + 6C_{112} + 12C_{144} + 24C_{166} + 2C_{123} + 16C_{456}}{9}$

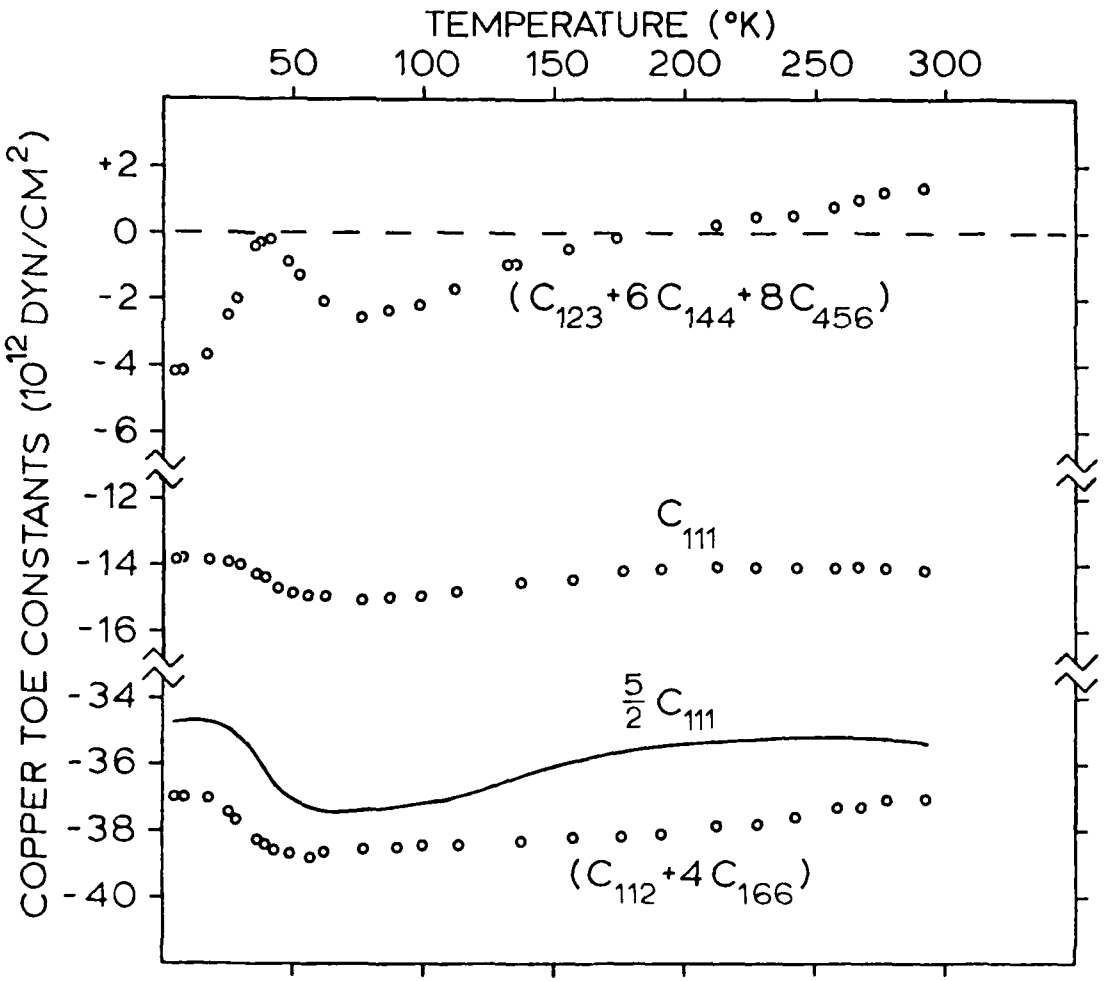

Figure 3. Simplest combinations of TOE constants plotted as a function of temperature.

origin of this effect can be located somewhat more exactly by examining Fig. 3, a plot of the simplest TOE constant combination available from our data.

The combinations of TOE constants in Fig. 3 happen to correspond to combinations which occur in the Hiki-Granato relations. One finds that the Hiki-Granato relations predict that

$$C_{112} + 4C_{166} = 5/2\ C_{111}$$

and $$C_{123} + 6C_{144} + 8C_{456} = 0.$$

Thus, on Fig. 3 we have plotted $5/2\ C_{111}$ to aid in the comparison. In Fig. 3 one finds that $C_{112} + 4C_{166} = 5/2\ C_{111}$ to within approximately 6% over the entire temperature range. We may also point out that the two curves have almost identical shapes over the entire temperature range, and this implies that

$$\frac{\partial C_{111}}{\partial T} = \frac{\partial (C_{112} + 4C_{166})}{\partial T} = \frac{\partial C_{112}}{\partial T} + 4\ \frac{\partial C_{166}}{\partial T}$$

over the same temperature range. This observation is consistent with the contentions of Hiki, Thomas, and Granato[19] that higher-order elastic constants of materials which have markedly overlapped closed shells are influenced most strongly by nearest neighbors.

The combination of TOE constants $(C_{123} + 6C_{144} + 8C_{456})$ exhibits an interesting behavior, becoming slightly positive above 200 °K. (This combination should be zero according to the central force, nearest neighbor model.) At all temperatures, it remains small in comparison to the other combinations. However, it exhibits a dip which

begins near 45 °K, reaches its minimum value near 75 °K and changes slope in the neighborhood of 200 °K. This behavior has the same general temperature dependence as the Bordoni peak in copper.[20] Perhaps this combination is sensitive to dislocation movement.

In conclusion, we feel that our data are nominally consistent with the predictions of a central forces, nearest neighbor interaction model. As usual, there are details which need to be explained, but further explanation would depend upon a more detailed model than we have used, and more detailed data than are available.

Acknowledgment

Research supported by the U.S. Office of Naval Research. The authors are grateful to R. D. Peters for his contribution to the data.

*Present address: Dept. of Physics, Emory & Henry College, Emory, VA 24327

**Present address: NASA Langley Research Center, Hampton, VA 23665.

1. W. B. Gauster and M. A. Breazeale, Rev. Sci. Instrum. 37, 1544 (1966).
2. R. D. Peters, M. A. Breazeale, and V. K. Paré, Rev. Sci. Instrum. 39, 1505 (1968).
3. R. D. Peters, M. A. Breazeale, and V. K. Paré, Phys. Rev. B 1, 3245 (1970).
4. W. T. Yost and M. A. Breazeale, Phys. Rev. B 9, 510 (1974).
5. J. A. Bains, Jr. and M. A. Breazeale, Phys. Rev. B 13, 3623 (1976).
6. John H. Cantrell, Jr. and M. A. Breazeale, Phys. Rev. B 17, 4864 (1978).
7. W. B. Daniels and C. S. Smith, Phys. Rev. 111, 713 (1958).
8. Y. Hiki and A. V. Granato, Phys. Rev. 144, 411 (1966).
9. K. Salama and G. A. Alers, Phys. Rev. 161, 673 (1967).
10. W. B. Gauster and M. A. Breazeale, Phys. Rev. 168, 655 (1968).
11. C. S. G. Cousins, J. Phys. C (Great Britain) 4, 1117 (1971).
12. M. A. Breazeale and Joseph Ford, J. Appl. Phys. 36, 3486 (1965).
13. W. C. Overton and John Gaffney, Phys. Rev. 98, 969 (1955).
14. E. Grüneisen, Ann. Phys. (Leipzig) 39, 257 (1912).
15. O. L. Anderson, Phys. Rev. 144, 553 (1966).
16. Y. A. Chiang, J. of Phys. and Chem. Solids 28, 697 (1967).
17. R. R. Rao, Phys. Rev. B 10, 4173 (1974).
18. John H. Cantrell, Jr., M. A. Breazeale, and A. Nakamura, J. Acoust. Soc. Am. (to be published); John H. Cantrell, Jr., Phys. Rev. (to be published).
19. Y. Hiki, J. F. Thomas, Jr., and A. V. Granato, Phys. Rev. 153, 764 (1967).
20. L. J. Bruner, Phys. Rev. 118, 399 (1960).

MEASUREMENT OF NONLINEARITY PARAMETERS IN SMALL SOLID SAMPLES BY THE HARMONIC GENERATION TECHNIQUE

M. A. Breazeale and Bruce Blackburn

Dept. of Physics, University of Tennessee, Knoxville, TN 37916, USA

We present results of examination of the ultrasonic harmonic generation technique for measurement of nonlinearity parameters, and hence the third order elastic constants, of solids. Heretofore, samples 2.5 cm in diameter and at least 2.5 cm in length have been used in measurements with a 1 cm diameter 30 MHz quartz transducer. Our results reveal that the minimum size of a sample which will allow accuracies between 5 and 10% in c_{ijk} measurements is 4 mm in ultrasonic path length and 5 mm in diameter. Correction of the data for diffraction effects is necessary with transducers or receivers smaller than 12.5 mm.

INTRODUCTION

A finite amplitude sinusoidal ultrasonic wave propagating through a nonlinear medium distorts as it propagates. This waveform distortion can be characterized as harmonic generation, and the measurement of the harmonic generation makes possible the evaluation of the nonlinearity parameters of the material. If the material is a cubic crystal, then one finds pure mode propagation along the principal directions. Measurement of the harmonic generation along the pure mode directions reduces to the measurement of the amplitude of the fundamental A_1 and of the second harmonic A_2, since the nonlinearity parameter is given by [1]

$$\beta = -\left(\frac{3K_2 + K_3}{K_2}\right) = \frac{8A_2}{A_1^2 k^2 a} \qquad (1)$$

where K_2 and K_3 are the linear combinations, respectively, of the second- and third-order elastic constants given in Table I, $k = 2\pi/\lambda$ is the propagation constant, and a is the propagation distance (sample length).

Table I. K_2 and K_3 for [100], [110], and [111] directions in cubic crystals

Direction	K_2	K_3
[100]	C_{11}	C_{111}
[110]	$\frac{C_{11} + C_{12} + 2C_{44}}{2}$	$\frac{C_{111} + 3C_{112} + 12C_{166}}{4}$
[111]	$\frac{C_{11} + 2C_{12} + 4C_{44}}{3}$	$\frac{C_{111} + 6C_{112} + 12C_{144} + 24C_{166} + 2C_{123} + 16C_{456}}{9}$

EXPERIMENTAL TECHNIQUE

The amplitudes of the fundamental and of the second harmonic are measured by use of

Reprinted from Proceedings of Ultrasonics International 1979, Graz, Austria, May 15-17, 1979, pp. 500-504.

the capacitive receiver shown in Fig. 1. Ultrasonic wave pulses are generated by the quartz transducer and propage downward through the sample and impinge on the bottom surface. Since the sample surfaces are optically flat, a receiver button can be placed at a distance S_0 from the sample to form a parallel plate capacitor. With a bias voltage V_b of approximately 150 volts dc, one finds that the ultrasonic wave impinging on the interface gives an ac voltage [2]

$$V = \frac{2AV_b}{S_0} \qquad (2)$$

where A is the amplitude of the harmonic to be measured.

Approximations

We have examined the approximations inherent in the use of harmonic generation to measure the nonlinearity parameters of solids and find that three of them need to be examined in order to define the smallest sample one can use:

(a) Infinite plane wave assumption,
(b) Parallel plate capacitor approximation,
(c) Effect of diffraction.

ANALYSIS OF MEASUREMENT TECHNIQUE

With the approximations in mind, one can evaluate the smallest sample size usable with present techniques:

(a) Infinite Plane Wave Assumption

In deriving Eq. (1), the assumption is made that the second harmonic is generated by a fundamental which is an infinitely extended plane wave. Although this is not strictly true in our experimental arrangement, as we will see, we can assume infinitely extended plane waves for the moment to estimate the minimum sample thickness required to produce measurable second harmonics. We have found that we can reliably measure second harmonics A_2 of the order of 10^{-3} Angstroms, and have measured 10^{-4} Angstroms. Using A_2 min = 10^{-4} Angstroms, and values of k_2 and k_3 for copper [11] as typical values, one finds that the minimum sample thickness a_{min} = 4 mm. In other materials different values of k_2 and k_3 might change this minimum thickness by a factor of two in either direction.

(b) Parallel Plate Capacitor Approximation

Equation (2) is strictly valid only if the capacitive receiver is effectively an infinitely extended parallel plate capacitor. In the experiments to be described, our smallest capacitor button had a diameter of 6.35 mm and a spacing of [illegible]. The ratio of diameter to spacing, then, is of the order of [illegible]. The effect of "fringing," which is to change the effective area of the plates, in this case is of the order of [illegible], which is negligible in our experiments. The diameter [illegible] be smaller by a factor of ten before the correction would be as large as [illegible]. Therefore, this approximation is not a major concern in our measurements.

(c) Effect of Diffraction

The effect of diffraction in finite amplitude experiments is not known in detail. Of course, one can solve diffraction problems in the linear approximation. But the effect of inclusion of nonlinear terms in the diffraction integral is difficult to evaluate mathematically.

Therefore, we have used the largest samples and the largest transducers [illegible]. A number of considerations led us to use cylindrical samples [illegible] in diameter and, typically, [illegible]. At a fundamental frequency of [illegible], transducers [illegible] cm in diameter give a [illegible] ratio of approximately [illegible].

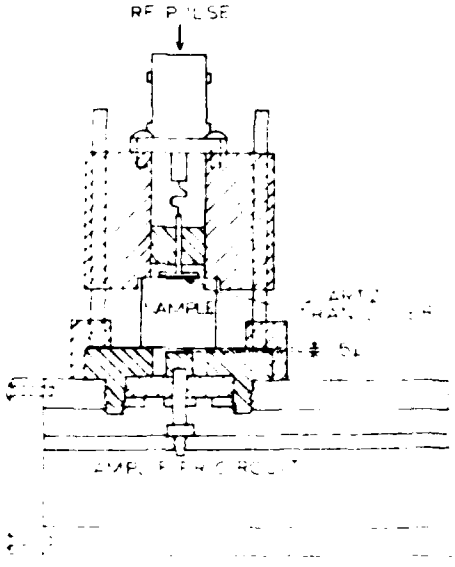

Figure 1. Capacitive receiver for measuring harmonic generation.

was assumed to satisfy the infinite plane wave assumption reasonably well in samples which were small enough to place in a helium cryostat.

EXPERIMENTAL RESULTS

We now would like to report the results of a systematic experimental investigation of the effect of diffraction on our measurements. A single crystal copper sample was selected which allowed ultrasonic wave propagation along the [111] direction. The sample was 2.54 cm in diameter and 3.96 cm in length. By selecting transducers with diameters given in Table II, we were able to effectively have the capacitive receiver in either the Fresnel zone or the Fraunhofer zone of the ultrasonic wave diffraction field. Two capacitive receivers were used with diameters of 11.8 and 6.36 mm.

Table II. Transducer diameters and ultrasonic beam characteristics used in a [111] copper sample. Receiver diameters were 11.8 and 6.36 mm.

Transducer Diameter (mm)	D/λ	a^2/λ (mm)	θ (degrees)
12.65	74	233	0.9
5.40	32	43	2.2
3.70	22	20	3.2
1.95	11	6	6.1

To give an idea of the relative size, a scale drawing of the (linear) ultrasonic wave field in the sample is given in Fig. 2. To make the drawing we have assumed that the intermediate size 3.70 mm transducer is behaving as a piston vibrator and is producing a beam whose half-angle θ is given by

$$\sin \theta = 0.61 \lambda/a \tag{3}$$

where λ is the (fundamental) ultrasonic wavelength and a is the transducer radius. The distance a^2/λ, sometimes referred to as the Fresnel distance, also is indicated. For the largest transducer this distance is much greater than the sample length so that the measurements are made within the Fresnel zone where the plane wave approximation is reasonably well-satisfied.

As seen from Eq. (1), a measure of the nonlinearity parameter for a given frequency and sample length is the ratio A_2/A_1^2. From Eq. (2), it is clear that this ratio is proportional to V_2/V_1^2 where V_1 and V_2 are the voltages generated in the receiver by the fundamental and the second harmonic, respectively. We would determine the effect on this measured quantity by diffraction. The averages of a number of measurements of the ratio V_2/V_1^2 are plotted as a function of the transducer diameter in Fig. 3. As indicated, we find that the measured V_2/V_1^2 values fall on smooth curves for each receiver size. At the moment there is no theoretical justification for this experimentally observed fact. However, there are some consistent observations which can be made.

The data point for the transducer-receiver combination heretofore used in measuring nonlinearity parameters is indicated by a solid point. It is reassuring to note that the asymptote of the curve for the smaller receiver button passes through the solid point. Because of the consistency of the data, one might assume that our data to date have been taken under conditions which reasonably well satisfy the theoretical assumptions, and thus do not require correction at this time. Further, the consistency of the curves suggest that smaller samples can be used than we have used heretofore. Specifically, data can be taken in samples so small that the plane wave assumption is not satisfied. It seems that curves similar to those in Fig. 3 can be used as calibration curves to evaluate from data taken with small samples the attenuation, α_2/α_1^2, and hence the nonlinearity parameter characteristic of a sample large enough to satisfy the infinite plane wave assumption. For example, the

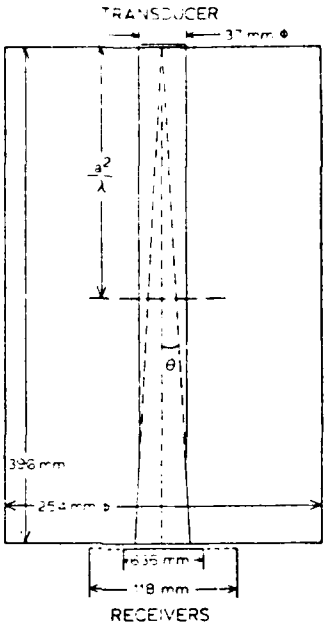

Figure 2. Ultrasonic wave field produced by 3.7 mm transducer.

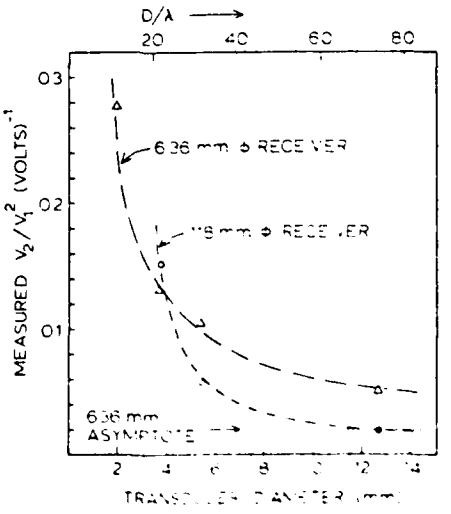

Figure 3. Measured values of the quantity V^2/V_1^2 for different transducer and receiver diameters.

data points at a transducer diameter of 3.7 mm require a correction to bring them in line with the value of V_2/V_1^2 indicated by the solid point, and the correction factor can be evaluated from the curves. Correction of data for smaller transducer diameters might not be accurate enough. Allowing the sample walls to be well outside the ultrasonic beam might require a sample diameter of, say, 5 mm. Thus, we come to an approximate answer to the question posed: the smallest sample usable with the harmonic generation technique has a diameter of 5 mm and a length of 4 mm. The surfaces must be optically flat and parallel, of course.

Finally, we would point out that a very promising prospect exists for progress in the general subject of nonlinear acoustics. Figure 3 is the first numerical evidence we have that after including the nonlinear terms describing the propagating medium, the diffraction integral should have solutions which are tractable. The curves give the values of an integral across a plane at specified distances from a sinusoidally vibrating piston source which is radiating into a nonlinear medium. A large number of such curves taken for different distances and different transducer sizes would allow one to evaluate directly the effect of diffraction on harmonic generation. This remains one of the unsolved fundamental problems of nonlinear acoustics.

ACKNOWLEDGMENT

Research supported in part by the Office of Naval Research.

1 Breazeale, M. A. and Ford, Joseph, 'Ultrasonic studies of the nonlinear behavior of solids', J. Appl. Phys., vol. 36 (1965), pp 3486-3490.

2 Gauster, W. B. and Breazeale, M. A., 'Detector for measurement of ultrasonic strain amplitudes in solids,' Rev. Sci. Instrum., vol. 37 (1966), pp 1544-1548.

3 Gauster, W. B. and Breazeale, M. A., 'Ultrasonic measurement of the nonlinearity parameters of copper single crystals,' Phys. Rev., vol. 168 (1968), pp 655-661; Peters, R. D., Breazeale, M. A., and Paré, V. K., 'Ultrasonic measurement of the temperature dependence of the nonlinearity parameters of copper,' Phys. Rev., B, vol. 1 (1970), pp 3245-3250; Yost, W. T. and Breazeale, M. A., 'Adiabatic third-order elastic constants of fused silica,' J. Appl. Phys., vol. 44 (1973), pp 1909-1910; Yost, W. T. and Breazeale, M. A., 'Ultrasonic nonlinearity parameters and third-order elastic constants of germanium between 300° and 77°K,' Phys. Rev. B, vol. 9 (1974), pp 510-516; Bains, James A., Jr. and Breazeale, M. A., 'TOE constants of germanium between 300°K and 3°K,' Phys. Rev. B, vol. 13 (1976), pp 3623-3630; Cantrell, John H., Jr. and Breazeale, M. A., 'An ultrasonic investigation of the nonlinearity of fused silica for different hydroxyl ion contents and homogeneities between 300 and 3 °K,' Phys. Rev. B, vol. 17 (1978), pp 4864-4870.

Relationship between solid nonlinearity parameters and thermodynamic Grüneisen parameters

John H. Cantrell, Jr.,[a] M. A. Breazeale, and Akira Nakamura[b]

Department of Physics, The University of Tennessee, Knoxville, Tennessee 37916
(Received 9 April 1979; accepted for publication 15 February 1980)

The relationship between the ultrasonic nonlinearity parameter for solids and the acoustic Grüneisen number has been derived for longitudinal ultrasonic wave propagation in the pure mode directions of cubic crystals and isotropic solids. Agreement between the acoustic Grüneisen number and the thermodynamic Grüneisen parameter is best for ultrasonic harmonic generation measurements along the [100] direction of a cubic crystal. Comparison of the temperature curves of the acoustic Grüneisen number of copper shows that the acoustic Grüneisen number generally follows the temperature dependence of the lattice contribution to the thermodynamic Grüneisen parameter.

PACS numbers: 43.25.Ba, 43.35.Cg

INTRODUCTION

In developing the harmonic generation technique for measurement of the nonlinear properties of solids, we have found a fundamental significance to the ratio of coefficients of the nonlinear terms to the linear terms in the nonlinear wave equation describing the propagation of a finite amplitude ultrasonic wave in the solid. This ratio, defined as the ultrasonic nonlinearity parameter for solids, is found[1] in the perturbation solution for the particle displacement, in the expression for the discontinuity distance, in the implicit solution for the wave velocity, etc. In addition, this quantity is observed to be only weakly dependent on temperature in those solids studied.[2-5] These observations have led us to realize that there is an intimate relationship between the ultrasonic nonlinearity parameter and the Grüneisen parameter evaluated, for example, from studies of Brillouin scattering,[6] from thermal expansion,[7] or from ultrasonic attenuation.[8] The purpose of the present work is to define the acoustic Grüneisen number for cubic crystals and isotropic solids and to give the relationship between it and the ultrasonic nonlinearity parameter. Values of the acoustic Grüneisen number taken from room temperature data on ultrasonic harmonic generation are presented, and a comparison is made between the temperature dependence of the acoustic Grüneisen number and that of the thermodynamic Grüneisen parameter.

I. THEORY

One can consider the wave equation in a cubic crystal for three pure-mode directions: [100], [110], and [111]. In these three directions pure longitudinal waves may propagate and the transverse wave is not excited. The nonlinear equation of motion for pure longitudinal waves in these three directions, assuming no attenuation, may be written

$$\rho_0 \frac{\partial^2 u}{\partial t^2} = K_2\left(\frac{\partial^2 u}{\partial a^2} + 3\frac{\partial u}{\partial a}\frac{\partial^2 u}{\partial a^2}\right) + K_3 \frac{\partial u}{\partial a}\frac{\partial^2 u}{\partial a^2}, \tag{1}$$

where ρ_0 is the unstrained mass density, u is the longitudinal displacement, and a is the Lagrangian coordinate along the wave propagation direction. K_2 and K_3 are linear combinations of second- and third-order elastic constants and are given in Table I for the three pure-mode directions in the cubic crystal. The equation of motion for an isotropic solid is identical to that of a cubic crystal in the [100] direction, with the appropriate interpretation of C_{11} and C_{111}. An implicit solution for the particle velocity $\partial u/\partial t$, which satisfies Eq. (1) and the boundary condition

$$\frac{\partial u}{\partial t} = \left(\frac{\partial u}{\partial t}\right)_{a=0} \sin \omega t \tag{2}$$

can be written in the form[1]

$$\frac{\partial u}{\partial t} = \left(\frac{\partial u}{\partial t}\right)_{a=0} \sin\left\{\omega t - \omega a\left[\left(\frac{K_2}{\rho_0}\right)^{-1/2} + \frac{1}{2}\left(\frac{K_2}{\rho_0}\right)^{-1}\left(\frac{3K_2 + K_3}{K_2}\right)\frac{\partial u}{\partial t}\right]\right\}. \tag{3}$$

In analogy with the results of Earnshaw[9] for gases, one finds that the phase velocity V_i can be written

$$V_i = V_{0i} + \frac{1}{2}\beta_i \frac{\partial u}{\partial t}, \tag{4}$$

where $V_{0i} = (K_2/\rho_0)^{1/2}$ is the velocity of a wave having infinitesimal amplitude and

TABLE I. K_2 and K_3 for [100], [110], and [111] directions.

Direction	K_2	K_3
[100]	C_{11}	C_{111}
[110]	$\frac{C_{11} + C_{12} + 2C_{44}}{2}$	$\frac{C_{111} + 3C_{112} + 12C_{166}}{4}$
[111]	$\frac{C_{11} + 2C_{12} + 4C_{44}}{3}$	$\frac{C_{111} + 6C_{112} + 12C_{144} + 24C_{166}}{9} + \frac{2C_{123} + 16C_{456}}{9}$

[a] Present address: NASA Langley Research Center, M.S 499 Hampton, VA 23665.

[b] Present address: Institute of Scientific and Industrial Research, Osaka University, Osaka, Japan.

 0001-4966/80/051477-03$00.80

TABLE II. Acoustic Grüneisen numbers γ_i^S for [100], [110], and [111] directions in cubic crystals.

Direction	γ_i^S
[100]	$-\left(\frac{3C_{11}+C_{111}}{2C_{11}}\right)$
[110]	$-\left(\frac{6C_{11}+6C_{12}+12C_{44}+C_{111}+3C_{112}+12C_{166}}{4C_{11}+4C_{12}+8C_{44}}\right)$
[111]	$-\left(\frac{9C_{11}+18C_{12}+36C_{44}+C_{111}+6C_{112}+12C_{144}+24C_{166}+2C_{123}+16C_{456}}{6C_{11}+12C_{12}+24C_{44}}\right)$

$$\beta_i = [(3K_2+K_3)/K_2]_i \tag{5}$$

is defined as the ultrasonic nonlinearity parameter for solids. The subscript i represents all indices specifying longitudinal wave propagation in the pure-mode directions of the crystal. The effect of the nonlinear terms in the wave equation, then, is to change the phase velocity by an amount proportional to the product of the particle velocity $\partial u/\partial t$ and the nonlinearity parameter β_i. This solution is valid for propagation distances less than the discontinuity distance

$$L_i = V_{0i}^2\left[\beta_i\omega\left(\frac{\partial u}{\partial t}\right)_{a=0}\right]^{-1}, \tag{6}$$

which is of the order of 1 m for common solids. From Eq. (4) and assuming irrotationality, the change in velocity, $\Delta V_i = V_i - V_{0i}$, resulting from the nonlinearity of the medium can be expressed in terms of the displacement gradient $\partial u/\partial a$ by

$$\Delta V_i = \frac{1}{2}\beta_i\frac{\partial u}{\partial t} = -\frac{1}{2}\beta_i V_{0i}\frac{\partial u}{\partial a}. \tag{7}$$

In order to relate this change in velocity to the change of thermal phonon velocity resulting from lattice anharmonicity, it is convenient to define the acoustic Grüneisen number specifying the adiabatic strain dependence of a lattice frequency ν_i for the longitudinal mode i by

$$\gamma_i^S = -\frac{1}{\nu_{0i}}\left(\frac{\partial \nu_i}{\partial(\partial u/\partial a)}\right)_S, \tag{8}$$

where the subscript S emphasizes the fact that the derivative is taken under isentropic conditions, and the subscript i represents all indices specified by longitudinal wave propagation in the directions [100], [110], and [111]. Here we take the derivative with respect to the displacement gradient $\partial u/\partial a$ rather than with respect to the Lagrangian strain measure as ordinarily is done in defining generalized Grüneisen parameters. This is possible because in harmonic generation experiments the nonlinearity parameter is obtained by extrapolating to zero amplitude a plot of the ratio of the amplitudes of the second harmonic to the square of the fundamental amplitude as a function of the fundamental amplitude. In the limit of zero amplitude the difference between the displacement gradient and the Lagrangian strain measure vanishes. When evaluated at zero strain, the acoustic Grüneisen number of Eq. (8) is the same as Brugger's tensorial isentropic Grüneisen number[10] for a longitudinal strain along the propagation direction of the mode.

According to the standing wave condition of the Debye continuum model, for any state of strain the mode frequencies are related to the wave speed V_i and the unstrained dimension l of the crystal by[10]

$$\nu_i \propto V_i/l. \tag{9}$$

Substituting this expression for the mode frequencies into Eq. (8) and integrating between V_{0i} and V_i, one obtains

$$V_i - V_{0i} = \Delta V_i = -\gamma_i^S V_{0i}\frac{\partial u}{\partial a}. \tag{10}$$

Comparing Eqs. (10) and (7) one finds the relationship between the acoustic Grüneisen number and the ultrasonic nonlinearity parameter for solids is expressed by

$$\gamma_i^S = \tfrac{1}{2}\beta_i. \tag{11}$$

In Table II are listed the acoustic Grüneisen numbers for the three pure-mode directions in cubic crystals.

II. COMPARISON WITH EXPERIMENT AND CONCLUSION

Ultrasonic nonlinearity parameters have been measured for germanium, copper, and fused silica. As

TABLE III. Comparison of adiabatic Grüneisen number and other Grüneisen parameters.

	γ_i^S Present work			Γ Nava and Romero[a]			γ Collins and White[b]
	$\gamma_{[100]}^S$	$\gamma_{[110]}^S$	$\gamma_{[111]}^S$	$\Gamma_{[100]}$	$\Gamma_{[110]}$	$\Gamma_{[111]}$	
Copper	2.64	5.50	3.94				2.00
Germanium	1.5	3.0	2.6	1.07	1.12	1.41	0.75
Fused silica	−5.8						0.18

[a] R. Nava and J. Romero, J. Acoust. Soc. Am. **64**, 529–532 (1978).

[b] J. G. Collins and G. K. White, "Thermal Expansion of Solids" in *Progress in Low Temperature Physics*, edited by C. J. Gorter (Wiley, New York, 1964), Vol. 4.

these measurements have been made from room temperature down to 3 °K, a fairly detailed comparison can be made between the acoustic Grüneisen number and other Grüneisen parameters in some cases.

In Table III we list room temperature values of the acoustic Grüneisen number. Also listed are room temperature values of thermodynamic Grüneisen parameters[7] and effective ultrasonic Grüneisen parameters. The thermodynamic Grüneisen parameter is given by

$$\gamma = \alpha/K_T C_V = \alpha/K_S C_P, \tag{12}$$

where α is the total thermal volume expansivity, K_T and K_S are the isothermal and the isentropic compressibilities, respectively, and C_V and C_P are the isochoric and isobaric heat capacities. The effective ultrasonic Grüneisen parameter Γ_P is related to the ultrasonic attenuation for a wave of polarization p and propagation direction q by[11]

$$\alpha_p = (3\Omega^2 K_q T/\rho C_p^3 S^2)\Gamma_P^2, \tag{13}$$

where K_q is the thermal conductivity along q, T is the absolute temperature, Ω is the ultrasonic angular frequency, ρ is the mass density, and C_p and S are the sound wave and Debye average velocities, respectively.

Examination of Table III reveals the fact that the acoustic Grüneisen number $\gamma^S_{[100]}$ agrees most closely with the thermodynamic Grüneisen parameter, and that all three of the acoustic Grüneisen numbers are larger in magnitude than the thermodynamic Grüneisen parameter. The greatest discrepancy between the two Grüneisen parameters occurs for fused silica for which the acoustic Grüneisen number is negative. Interestingly enough, the behavior is consistent, for fused silica exhibits an anomalous behavior of many of its thermodynamic and ultrasonic properties.[12-14] The negative value of the acoustic Grüneisen number is related to the fact that the second harmonic in fused silica is generated 180° out of phase with that generated in other solids.[15]

It is significant that the agreement between the acoustic Grüneisen numbers and the effective ultrasonic Grüneisen parameters of germanium is as good as it is, because the data come from fundamentally different measurements: ours from harmonic generation, Nava and Romero's from attenuation.

The temperature dependence of the acoustic Grüneisen number for the [100] direction in single crystal copper was found to be quite similar to that of the thermodynamic Grüneisen parameter. The two are plotted on the same graph in Fig. 1. The temperature scale is the reduced temperature T/θ, where the Debye temperature $\theta = 345$ °K for copper. A smooth curve is drawn through experimental values of $\gamma^S_{[100]}$. For comparison, values of the thermodynamic Grüneisen parameter[7] are plotted on the same graph. The total Grüneisen parameter is indicated by a solid curve. In the low temperature region the electronic contribution to the thermodynamic Grüneisen parameter is distinguishable. The dotted curve labeled "l" for "lattice" contribution remains essentially constant, while the total curve labeled "$l+e$" for "lattice plus electron" decreases as the temperature is lowered.

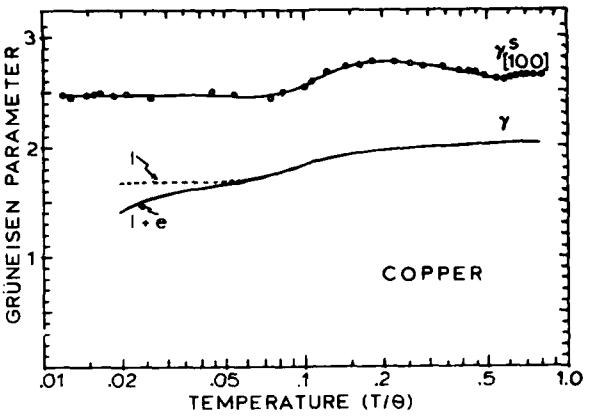

FIG. 1. Temperature dependence of the acoustic Grüneisen number $\gamma^S_{[100]}$ and the thermodynamic Grüneisen parameter γ of copper.

It is interesting to notice that the acoustic Grüneisen number $\gamma^S_{[100]}$ remains parallel to the lattice contribution to the thermodynamic Grüneisen parameter, and almost exactly 1.5 times as large. The significance of this observation is under investigation at the present time.

ACKNOWLEDGMENTS

This research was supported in part by the U. S. Office of Naval Research. The authors wish to thank Dr. W. T. Yost of Emory and Henry College for his help in taking and analyzing the experimental data for the copper samples.

[1] M. A. Breazeale and J. Ford, J. Appl. Phys. **36**, 3486–3490 (1965).
[2] R. D. Peters, M. A. Breazeale, and V. K. Paré, Phys. Rev. B **1**, 3245–3250 (1970).
[3] W. T. Yost and M. A. Breazeale, Phys. Rev. B **9**, 510–516 (1974).
[4] J. A. Bains, Jr., and M. A. Breazeale, Phys. Rev. B **13**, 3623–3630 (1976).
[5] J. H. Cantrell, Jr., and M. A. Breazeale, Phys. Rev. B **17**, 4864–4870 (1978).
[6] W. Heinicke, G. Winterling, and K. Dransfeld, J. Acoust. Soc. Am. **49**, 954–958 (1971).
[7] J. G. Collins and G. K. White, "Thermal Expansion of Solids," in *Progress in Low Temperature Physics*, edited by C. J. Gorter (Wiley, New York, 1964), Vol. 4.
[8] R. Nava and J. Romero, J. Acoust. Soc. Am. **64**, 529–532 (1978).
[9] S. Earnshaw, Phil. Trans. Soc. (London) **150**, 133 (1860).
[10] K. Brugger, Phys. Rev. **137**, A1826–A1827 (1965).
[11] R. Nava, M. P. Vecchi, J. Romero, and B. Fernández, Phys. Rev. B **14**, 800–807 (1976).
[12] P. Flubacher, A. J. Leadbetter, J. A. Morrison, and B. P. Stoicheff, J. Phys. Chem. Solids **12**, 53–65 (1959).
[13] A. E. Clark and R. E. Strakna, Phys. Chem. Glasses **3**, 121–126 (1962).
[14] G. K. White and J. A. Birch, Phys. Chem. Glasses **6**, 85–89 (1965).
[15] J. A. Bains, Jr., and M. A. Breazeale, J. Acoust. Soc. Am. **57**, 745–746 (1975).

QUANTUM MECHANICAL THEORY OF NONLINEAR INTERACTION OF ULTRASONIC WAVES

Ivan L. Bajak[a] and M. A. Breazeale
Department of Physics
The University of Tennessee
Knoxville, TN 37916

ABSTRACT

Nonlinear interaction of ultrasonic waves is discussed from the very general quantum mechanical viewpoint. By using the concept of three-phonon interactions one is able to derive formulae for power and intensity of ultrasonic waves generated through nonlinear mixing of two ultrasonic waves, as well as the formula for parametric amplification of an ultrasonic wave through its nonlinear interaction with another ultrasonic wave. The effect of attenuation on nonlinear ultrasonic wave interactions also is discussed, and it is shown that in some situations attenuation strongly affects the generation of the second harmonic of an initially sinusoidal ultrasonic wave. It is shown that in the correspondence limit the quantum mechanical viewpoint gives results which are in very good agreement with results obtained from classical physics.

Will be published in November 1980 issue of Journal of the Acoustical Society of America.

I. INTRODUCTION

Nonlinear interactions of ultrasonic waves in solids are of two general types. First is the interaction in which two waves generate a third wave (this also includes harmonic generation of an initially sinusoidal wave, as we will see). Second is the amplification of an ultrasonic wave through its interaction with another ultrasonic wave. Taken together, these two types of nonlinear interaction offer a wide range of prospects of technical application in addition to providing an excellent possibility to study the fundamental anharmonicity of a crystalline lattice.

Theoretical discussion of the subject can be either from the classical approach or the quantum mechanical approach. In the classical approach one uses coupled-mode equations[1-6] and the classical language of "plane waves propagating in a semi-infinite medium." In spite of the fact that classical physics is quite adequate for discussion of ultrasonic interactions in which quantum effects are negligible, the quantum mechanical approach using the concept of phonons also has been applied to this problem.[7-12] The quantum mechanical approach gives a reasonably straightforward solution even when the interaction is treated as a three-dimensional problem in an anisotropic medium.

In general, the advantages of the quantum mechanical point of view in the description of ultrasonic wave interactions have not been utilized fully. Occasionally discrepancies occur in the results obtained by different authors,[7,11] and often there is difficulty in comparing different theoretical results because the definitions of the physical parameters are not totally consistent. Such nonuniformity of the theoretical approach tends to discourage comparison between experimental results on the nonlinear behavior of ultrasonic waves and results of quantum mechanical theories.

The present paper, therefore, is devoted to a unified quantum mechanical discussion of the nonlinear behavior of ultrasonic waves in crystals. We discuss both noncollinear and collinear interactions of ultrasonic waves and point out the possibility to measure nonlinear constants of the propagating medium. We employ the quantum mechanical treatment using the concept of phonons and show that the quantum mechanical treatment gives not only results obtained previously by classical methods, but also gives the possibility to describe very general cases of interaction of ultrasonic waves in an anisotropic medium of finite size.

In describing the nonlinear behavior of ultrasonic waves using the concept of three-phonon interaction, the very first problem is the derivation of the interaction Hamiltonian density operator. Section II is devoted to this derivation. Section III describes interactions in which two ultrasonic waves, through nonlinear mixing, generate an ultrasonic wave whose frequency is the sum of the frequencies of the mixed waves (parametric up-conversion). Section IV discusses parametric down-conversion of two ultrasonic waves and parametric amplification of an ultrasonic wave through its interaction with another ultrasonic wave. In Section V we consider the effect of attenuation in nonlinear interactions of ultrasonic waves. Finally, in Section VI we discuss the effect of our limiting assumptions and relate them to assumptions made in classical theories.

II. INTERACTION HAMILTONIAN

The interaction Hamiltonian density operator for three-phonon interactions can be obtained by starting with the classical form of the energy of interaction between two ultrasonic waves. First, one replaces the classical displacement vector by the corresponding operator. The components of the displacement operator then have the form:[13]

$$\hat{u}_i = \left(\frac{\hbar}{2\rho V\omega_q}\right)^{1/2}\left(\hat{a}_q e^{i\vec{q}\cdot\vec{r}} + \hat{a}_q^* e^{-i\vec{q}\cdot\vec{r}}\right)k_i^{(q)} \tag{1}$$

where $\hbar$ is Planck's constant divided by 2π; ρ is the mass density; V is the volume of normalization; ω_q is the angular frequency of a phonon having the wave vector $\vec{q}$; $\hat{a}_q$ and $\hat{a}_q^*$ are respectively the annihilation and the creation operators of the considered phonons; and $k_i^{(q)}$ are components of the polarization vector

$$\vec{k}^{(q)} = \frac{\vec{u}_o^{(q)}}{u_o^{(q)}},$$

where $\vec{u}_o^{(q)}$ is the amplitude of the ultrasonic wave. As the phonon of wave vector $\vec{q}$ in general can have three different polarizations, the index "q" will be understood to be a double index, referring both to wave vector and to polarization. Here, and in what follows, the Einsteinian summation over repeated indices will be understood.

Next, the classical form of an interaction energy density for the scattering of an ultrasonic wave S_{ij} by an ultrasonic wave S'_{ij} can be obtained if we assume that the wave S'_{ij} modulates the properties of the medium in which the wave S_{ij} is propagating. Thus, the energy density of the wave S_{ij} has the form

$$U = \left|\frac{1}{2}\left(C_{ijk\ell} + \frac{\partial C_{ijk\ell}}{\partial S_{mn}} S'_{mn}\right) S_{ij} S_{k\ell}\right| \tag{2}$$

where the S_{ij} and the S'_{ij} are the strain tensor components of the given ultrasonic waves and the $C_{ijk\ell}$ are the elastic moduli of the medium stiffened by the presence of an ultrasonic wave.

Using relations (1) and (2) and making a plane wave expansion, brings the Hamiltonian density to the form

$$\begin{aligned}\hat{H}_{int} = -\frac{i}{2}\left(\frac{\hbar}{2\rho V}\right)^{3/2}\Bigg\{ & C_{ijk\ell} m_i^{(q)} m_j^{(q')} m_k^{(q'')} k_\ell^{(q'')} \quad (\vec{k}^{(q)} \cdot \vec{k}^{(q')}) \\ & + \frac{\partial C_{ijk\ell}}{\partial S_{mn}} m_i^{(q)} m_k^{(q')} m_m^{(q'')} k_j^{(q)} k_\ell^{(q')} k_n^{(q'')}\Bigg)\left(\frac{\omega_q \omega_{q'} \omega_{q''}}{v_q^2 v_{q'}^2 v_{q''}^2}\right)^{1/2} \\ & \times \left(\hat{a}_q e^{i\vec{q}\cdot\vec{r}} - \hat{a}_q^* e^{-i\vec{q}\cdot\vec{r}}\right)\left(\hat{a}_{q'} e^{i\vec{q}'\cdot\vec{r}} - \hat{a}_{q'}^* e^{-i\vec{q}'\cdot\vec{r}}\right) \\ & \left(\hat{a}_{q''} e^{i\vec{q}''\cdot\vec{r}} - \hat{a}_{q''}^* e^{-i\vec{q}''\cdot\vec{r}}\right)\end{aligned} \tag{3}$$

where v_q, $v_{q'}$ and $v_{q''}$ are phase velocities of the phonons $(\vec{q},\omega_q)$, $(\vec{q}',\omega_{q'})$ and $(\vec{q}'',\omega_{q''})$ respectively, and $m_i^{(q)}$, $m_i^{(q')}$, and $m_i^{(q'')}$ are components of the unit vectors $\vec{m}^{(q)} = \vec{q}/q$, $\vec{m}^{(q')} = \vec{q}'/q'$ and $\vec{m}^{(q'')} = \vec{q}''/q''$. The first part of the interaction Hamiltonian density (3) arises as a result of the nonlinearity of the strain tensor and it expresses self-coupling of phonons; the second part of (3) is a consequence of the anharmonicity of the lattice.[14] In this form, the Hamiltonian density describes two kinds of three-phonon processes: First, the creation of a phonon through the annihilation of two phonons is suggested by those terms in Eq. (3) which contain $\hat{a}_q$, $\hat{a}_{q'}$, and $\hat{a}^*_{q''}$; second, the disintegration

of a phonon and the simultaneous creation of two new phonons is suggested by terms containing $\hat{a}_q$, $\hat{a}^*_q$, and $\hat{a}^*_{q_1}$.

In the following we discuss both processes and show their macroscopic behavior in the nonlinear interactions of ultrasonic waves.

III. PHONON CREATION THROUGH ANNIHILATION OF TWO PHONONS (Nonlinear Parametric Up-Conversion)

In a nonlinear medium two phonons can interact to create a new phonon. The experimental situation corresponding to this process is the situation in which two ultrasonic waves of angular frequency ω_1 and ω_2 generate a new ultrasonic wave of angular frequency $\omega_3 = \omega_1 + \omega_2$.

In describing the main features of this interaction, we will need knowledge of the size and shape of the interaction volume. In order to keep our discussion general, but also fairly simple, we shall assume that the interaction volume and the volume of normalization coincide with the volume of the sample under investigation. The interaction coupling constant $G_{q_1 q_2 q_3}$, however, will be assumed to have nonzero value only in that part of the sample in which the interaction actually takes place. This assumption can be employed if the considered part of the sample is much larger than the wavelength of the ultrasonic wave.

Let us now assume that there are N_1 phonons having the wave vector $\vec{q}_1$ and N_2 phonons having the wave vector $\vec{q}_2$ in the volume of the sample. Let us also assume that the initial state of the newly created phonons having the wave vector $\vec{q}_3$ is empty. This means that the initial state vector is $|N_1, N_2, 0\rangle$. The probability amplitude for transition from this initial state to the final state $\langle N_1 - 1, N_2 - 1, 1|$ is

$$\langle N_1-1,\ N_2-1,\ 1|\hat{H}_{int}|N_1,\ N_2,0\rangle = -i\left(\frac{\hbar}{2\rho V}\right)^{3/2} G_{q_1q_2q_3} \frac{(\omega_1\omega_2\omega_3)^{1/2}}{(v_1^2v_2^2v_3^2)}$$

$$\times \left(N_1N_2\right)^{1/2} \int_{(V_i)} e^{i(\vec{q}_1+\vec{q}_2-\vec{q}_3)\cdot\vec{r}}\, dV_i \qquad (4)$$

where V_i, the interaction volume, is the volume in which $G_{q_1q_2q_3}$ is assumed to have nonzero value. The quantity $G_{q_1q_2q_3}$ has the form

$$G_{q_1q_2q_3} = C_{ijk\ell}\Big\{ m_i^{(q_1)} m_j^{(q_2)} m_k^{(q_3)} k_\ell^{(q_3)} (\vec{k}^{(q_1)}\cdot\vec{k}^{(q_2)})$$

$$+ m_i^{(q_1)} m_j^{(q_3)} m_k^{(q_2)} k_\ell^{(q_2)} (\vec{k}^{(q_1)}\cdot\vec{k}^{(q_3)})$$

$$+ m_i^{(q_2)} m_j^{(q_3)} m_k^{(q_1)} k_\ell^{(q_1)} (\vec{k}^{(q_2)}\cdot\vec{k}^{(q_3)})$$

$$+ A_{ijk\ell mn} m_i^{(q_1)} m_k^{(q_2)} m_m^{(q_3)} k_j^{(q_1)} k_\ell^{(q_2)} k_n^{(q_3)}\Big\} \qquad (5)$$

where $(\vec{k}^{(q_1)}\cdot\vec{k}^{(q_2)})$ is the cosine of the angle between the polarization vectors $\vec{k}^{(q_1)}$ and $\vec{k}^{(q_2)}$, etc.

In deriving the probability amplitude, Eq. (4), we have assumed that $N_1>>1$, and $N_2>>1$. A factor 3! is implicit in Eq. (4) as a consequence of the summation over all possible q, q′, and q′′. The vectors $\vec{q}_1$ and $\vec{q}_2$ are fixed by the experimental situation, and the transition probability amplitude is to be considered a function of $\vec{q}_3$. The variability of $\vec{q}_3$, however, is limited by the integral

$$\Gamma = \int_{(V_i)} e^{i(\vec{q}_1+\vec{q}_2-\vec{q}_3)\cdot\vec{r}}\, dV_i \qquad (6)$$

which has, for an infinitely large volume V_1, a non-zero value only when $\vec{q}_3 = \vec{q}_1 + \vec{q}_2$. In case the volume V_1 is finite, the integral Γ has a non-zero value also when $\vec{q}_3 \neq \vec{q}_1 + \vec{q}_2$; i.e., when the law of conservation of momentum of interacting quasi particles is not fulfilled exactly.

The function Γ depends on the actual shape and size of the volume V_1, the part of the sample in which interaction actually takes place. Therefore, for a detailed treatment, the value of Γ should be calculated for each experimental situation separately. In the general case such effects as conical refraction[17] would complicate the calculation somewhat. For many experimental situations, however, it is adequate to proceed as follows.

We assume that V_1 is a parallelepiped with edges parallel to the x-, y-, and z-axes are L_x, L_y, and L_z. We call $\Delta\vec{q} = \vec{q}_1 + \vec{q}_2 - \vec{q}_3$ the misalignment vector and put $\frac{\Delta q_x L_x}{2} = a_x$, $\frac{\Delta q_y L_y}{2} = a_y$, and $\frac{\Delta q_z L_z}{2} = a_z$. For this case Γ we get

$$\Gamma = V_1 \frac{\sin a_x}{a_x} \frac{\sin a_y}{a_y} \frac{\sin a_z}{a_z}$$

which shows that for this finite volume V_1, the integral Γ also has a non-zero value when $\Delta\vec{q} \neq 0$, i.e., for $\vec{q}_1 + \vec{q}_2 \neq \vec{q}_3$.

The partial transition probability rate of the transition under consideration can now be expressed in the form

$$\frac{dP_1^f}{dt} = \frac{\pi\hbar}{4\rho^3 V^3} G^2 q_1 q_2 q_3 \Gamma^2 \frac{\omega_1\omega_2\omega_3}{v_1^2 v_2^2 v_3^2} N_1 N_2 \delta(\omega_1+\omega_2-\omega_3) \qquad (8)$$

In order to get the total transition probability rate we must sum all the partial probability rates, Eq. 8, over all possible final states of phonons $\vec{q}_3$, s_3. This means we must integrate Eq. 8 over all possible states of phonons $\vec{q}_3$, s_3. With the x-axis parallel to $(\vec{q}_1+\vec{q}_2)$, the total transition probability rate is

$$\frac{dT_1^f}{dt} = \iint \left[\frac{dP_1^f}{dt}\right] \left[\frac{V_3}{(2\pi)^3}\right] \frac{\omega_3^2}{v_3^3} d\omega_3 d\Omega \quad ,$$

where $d\Omega = d\theta_y d\theta_z$ is the space angle. The integral over the space angle can be evaluated if we know Eq. 9 as a function of the angles θ_y and θ_z, which are the deviations of $\vec{q}_3$ from the direction $\vec{q}_1 + \vec{q}_2$ in, respectively, the (x,y) plane and the (x,z) plane. It enters Eq. 8 through the integral Γ, which is expressed for the finite volume V_1 by Eq. 9.

In order to perform the integral over the space angle, we put $\Delta q_y = q_3\theta_y$, $\Delta q_z = q_3\theta_z$, and $\Delta q_x = 0$. In putting $\Delta q_x = 0$, we specify that $|\vec{q}_3|$ is a constant whose value is determined by simultaneous fulfillment of the law of conservation of energy and the law of conservation of momentum of the interacting quasi-particles. Now, using Eq. 9, we can write

$$\int_{-\pi}^{+\pi}\int_{-\pi}^{+\pi} d\theta_y d\theta_z = \frac{4V_1^2\pi^2}{L_y L_z q_3^2} \tag{10}$$

where we have taken into account the fact that Γ decreases rapidly with increasing θ and that the relations $\Delta q_y = q_3\theta_y$ and $\Delta q_z = q_3\theta_z$ can be used for large angles with negligible error. When L_y and L_z are much larger than the wavelength of the phonons with wave vectors $\vec{q}_1$, $\vec{q}_2$, we can assume that $\pi^2 L_y L_z / q_3^2$ is very large and then we can replace the sum $\sum_{-\pi}^{+\pi}$ by $\int_{-\infty}^{+\infty} dx = \pi$.

Using Eq. 10, the total transition probability rate becomes

$$\frac{dP}{dt} = \frac{\pi}{V_1^2 N_1 N_2} \sum_{\vec{q}_1,\vec{q}_2} q_3 \Gamma(\vec{q}_1,\vec{q}_2,\vec{q}_3) \frac{1}{v_1 v_2 v_3} N_1 N_2 \tag{11}$$

where dP/dt is the number of transitions per unit time. This means that the number of transitions in the volume V_1 is $V_1 N_3 dt$, where N_3 is the number of phonons with wave vector $\vec{q}_3$.

In the following we shall discuss some special examples of ultrasonic interactions. In preparation for this discussion we must realize that phonons $(\vec{q}_3,\omega_3)$ produced in the volume V_i are scattered from this volume principally along the direction $\vec{q}_1 + \vec{q}_2$. Therefore, we can obtain the power of the generated wave simply by multiplying Eq. 11 by $\hbar\omega_3$.

Noncollinear Interactions of Ultrasonic Waves

The power of the wave $(\vec{q}_1,\omega_1)$ is $(\hbar\omega_1 L_y L_z v_1 N_1/V)$, and the power of the wave $(\vec{q}_2,\omega_2)$ is $(\hbar\omega_2 L_y L_z v_2 N_2/V)$. Using these expressions and multiplying Eq. 11 by $\hbar\omega$ we can express the power of the wave generated by the noncollinear interaction of $(\vec{q}_1,\omega_1)$ and $(\vec{q}_2,\omega_2)$ as

$$P_3 = \frac{V_i^2}{L_y^3 L_z^3} \frac{G^2 q_1 q_2 q_3}{8\rho^3} \frac{\omega_3^2}{v_1^3 v_2^3 v_3^3} P_1 P_2 \qquad (13)$$

The wave of power P_3 is scattered from the volume V_i principally along the x-direction which is parallel to $\vec{q}_1 + \vec{q}_2$. By examining the relations (7) and (8), it can be shown that most of the phonons $(\vec{q}_3,\omega_3)$ are scattered into the solid angle given by the first minimum of the function Γ. The angular positions of these minima are given by $\theta_y^{(max)} = \pm \frac{2\pi}{q_3 L_y}$ and $\theta_z^{(max)} = \pm \frac{2\pi}{q_3 L_z}$, so that the solid angle in which most of the phonons are observed is

$$d\Omega = \frac{16\pi^2}{q_3^2 L_y L_z} . \qquad (13)$$

At large distances $R \gg L_y, L_z$, the average intensity of the wave scattered from the volume V_i can be calculated as

$$I_3 = \frac{V_i^2}{R^2} \frac{G^2 q_1 q_2 q_3}{128\pi^2 \rho^3} \frac{\omega_3^4}{v_1^3 v_2^3 v_3^5} I_1 I_2 \tag{14}$$

where I_1 and I_2 are the intensities of the two interacting waves (q_1,ω_1) and (q_2,ω_2). The apparent difference between (12) and (14) must be considered carefully when experimental data are taken.

For comparison with experiment we shall derive the formula for the amplitude of the ultrasonic wave $(\vec{q}_3,\omega_3)$. Using relations (7) and (8) and putting $a_x = 0$, $a_y = q_3\theta_y L_y/2$, and $a_z = q_3\theta_z L_z/2$, the transition probability rate for scattering of phonons $(\vec{q}_3,\omega_3)$ into a certain solid angle $\Delta\Omega$ is given by

$$\Delta P(\theta_y,\theta_z) = \frac{\pi G^2 q_1 q_2 q_3}{32\pi^2 \rho^3} \frac{\omega_1 \omega_2 \omega_3^3}{v_1^2 v_2^2 v_3^5} N_1 N_2 \frac{V_i^2 \sigma^2(\theta_y,\theta_z)}{V^2} \Delta\Omega \tag{15}$$

where

$$\sigma^2(\theta_y,\theta_z) = \left(\frac{\sin q_3\theta_y L_y/2}{q_3\theta_y L_y/2}\right)^2 \left(\frac{\sin q_3\theta_z L_z/2}{q_3\theta_z L_z/2}\right)^2 \tag{16}$$

Equation (15) gives the average number of phonons $(\vec{q}_3,\omega_3)$ scattered per unit of time into the solid angle $\Delta\Omega$ along the direction determined by the deviation angles θ_y and θ_z. Thus, by multiplying Eq. (15) by $\hbar\omega_3$ and dividing it by $R^2\Delta\Omega$, one can calculate the average intensity of the scattered wave at a distance R from the interaction volume. From this, one can obtain the amplitude of the ultrasonic wave in the form

$$A_3(\theta_y,\theta_z) = \frac{G_{q_1q_2q_3}}{8\pi\rho v_3^2} q_1q_2q_3A_1A_2 \frac{V_i\sigma(\theta_y,\theta_z)}{R} \tag{17}$$

This formula gives the distribution of the amplitude of the generated wave as a function of θ_y and θ_z. It gives an excellent possibility to analyze experimental data in detail and to correct for geometrical diffraction of the generated wave.

It is interesting to compare Eq. 17 with similar formulae obtained in references 9 and 11. Agreement is obtained if we put into Eq. 17, $\sigma = 1$ and $R = \sqrt{\frac{S}{4\pi}}$, where S is the cross sectional area of the wavefront. However, making this substitution eliminates the "wave" character of the scattering, and thus leads to inexactness. The results in 9 and 11 are inexact in that the scattering process has been calculated as though it were spherically isotropic scattering with strict fulfillment of the law of conservation of momentum. No such assumption is made in deriving Eq. 17.

Collinear Interactions: Second and Third Harmonic Generation by Sinusoidal Ultrasonic Waves

Collinear interactions of ultrasonic waves bring some peculiarities to the problem of correct interpretation of the theoretical formula because the created phonons $(\vec{q}_3,\omega_3)$ remain in the interaction volume: their phase velocity and direction of propagation are the same as the phase velocity and direction of propagation of the interacting waves (we neglect the effect of dispersion). First, we recall that the optimum conditions for interactions are given by simultaneous fulfillment of the laws of conservation of energy and of momentum. The corresponding relation can be written symbolically as

$$(\vec{q}_1,\omega_1) + (\vec{q}_2,\omega_2) = (\vec{q}_3,\omega_3) \ . \tag{18}$$

We can now introduce the symbolical vector $\vec{\omega}_n \equiv (\vec{q}_n,\omega_n)$, and using it we can graphically solve the relation (18) in the (q,ω) plane as shown in Figure 1. Dashed lines in Figure 1 should be drawn so that the tangent of the angle of deviation from the q-axis is equal to the corresponding phase velocity. Thus, using a diagram like Figure 1, it can be shown that collinear interaction can exist when the interacting waves have the same phase velocities, or only in special cases when the phase velocities are different; i.e., when $v_1 \neq v_2 \neq v_3$. This relation can be satisfied only in directions in a crystal which are not pure-mode directions. Thus, collinear interaction of waves of different modes can exist only when the waves are propagating along a direction which is not a pure-mode direction.

Let us now consider the case when $v_1 = v_2 = v_3$; i.e., the collinear interaction of waves of identical modes of polarization. The experimental situation in this case can be described as follows: Two ultrasonic pulses $(\vec{q}_1,\omega_1)$ and $(\vec{q}_2,\omega_2)$ are simultaneously launched into the sample at time $t = 0$. The pulses travel along a pure mode direction in the sample producing phonons $(\vec{q}_3,\omega_3)$ which remain in the space simultaneously occupied by both pulses, as we have assumed $v_1 = v_2 = v_3$. Describing this situation in terms of continuous waves, we can say that the concentration (number per unit volume) of phonons $(\vec{q}_3,\omega_3)$ at time $t = L_x/v_3$ produced in the pulse regime will be the same as the concentration produced by continuous waves propagating a distance L_x. Using this conclusion and using Eq. 11 for the concentration of phonons $(\vec{q}_3,\omega_3)$ at a distance L_x, we obtain

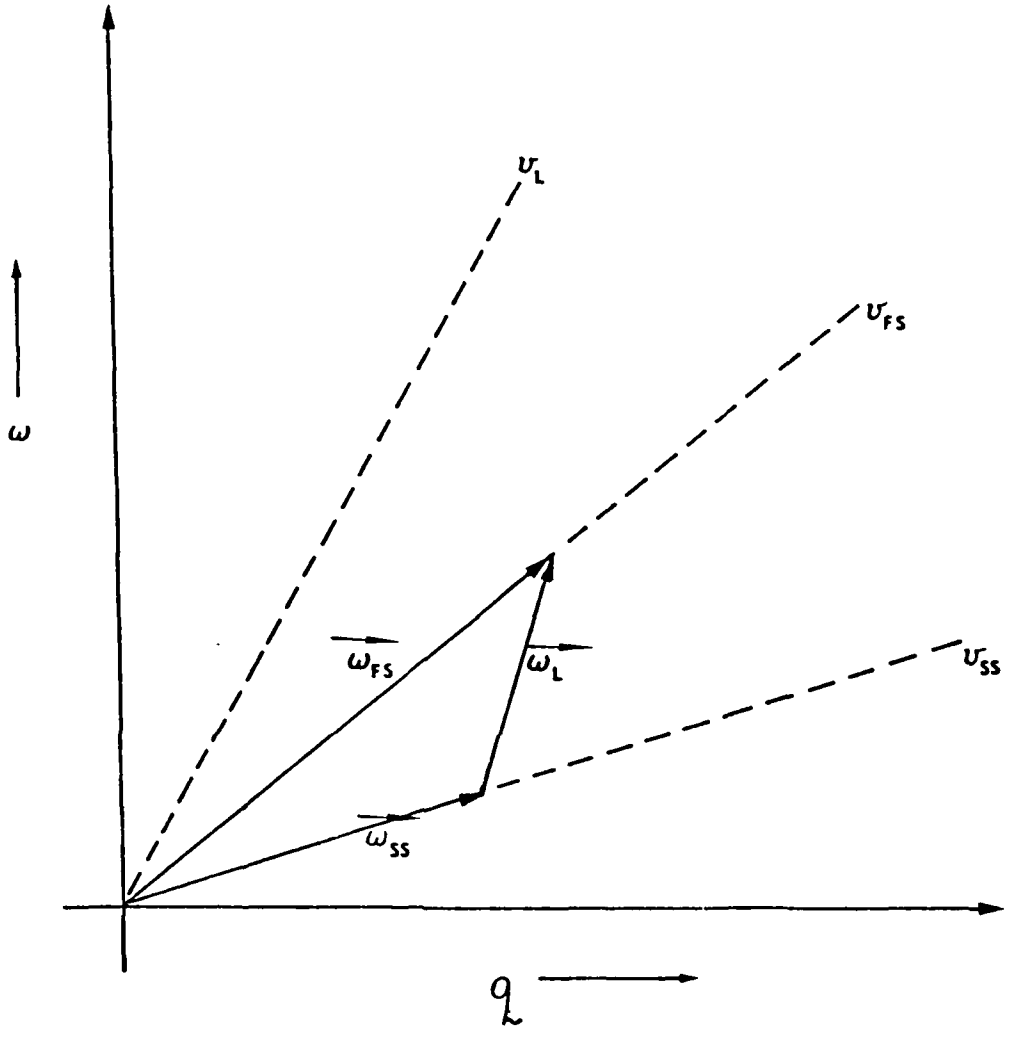

Figure 1. Vector diagram for simultaneous fulfillment of the laws of conservation of energy and of momentum.

$$N_3(L_x) = \frac{\hbar G^2_{q_1q_2q_3}}{8\rho^3 v^8}\,\omega_1\omega_2\omega_3 N_1 N_2 L_x^2 \tag{19}$$

where $v = v_1 = v_2 = v_3$. Realizing that $\hbar\omega N_i$ is the energy density of phonons in the wave identified by the subscript i, one can calculate the amplitude of the wave at the distance L_x as

$$A_3(L_x) = \frac{G_{q_1q_2q_3}}{4\rho v^2}\,q_1 q_2 A_1 A_2 L_x \tag{20}$$

In deriving both $N_3(L_x)$ and $A_3(L_x)$ we have assumed that N_1 and N_2 are constants and that $N_3 = 0$ at $t = 0$.

Second Harmonic Generation

Equations 19 and 20 can be applied directly to second harmonic generation by an initially sinusoidal ultrasonic wave. Simply putting $N_1 = N_2 = N_0/2$ and assuming $v_1 = v_2 = v_3 = v$ as before, we find that the second harmonic generated by a wave which has a concentration of phonons N_0 is, from Eq. 19:

$$N_s = \frac{\hbar G^2_{q_1q_2q_3}}{32\rho^3 v^8}\,\omega_o^2\omega_s N_o^2 L_x^2 \tag{21}$$

where N_S is the concentration of phonons in the second harmonic, while $\omega_S = 2\omega_0$ is its angular frequency. In a similar manner, from Eq. 20 one finds that the amplitude of the second harmonic at a distance L_x from the beginning of the sample is

$$A_s = \frac{G_{q_1 q_2 q_3}}{8\rho v^2} q_o^2 A_o^2 L_x \ . \qquad (22)$$

This formula agrees with that derived from classical considerations.[1] In Ref. 1, the amplitude of the second harmonic is given as $-(\frac{3K_2+K_3}{8K_2})A^2k^2a$, where K_2 and K_3 are the appropriate combinations of second-order and third-order elastic constants, respectively, A is the initial fundamental amplitude, k is the propagation constant $2\pi/\lambda$, and a is the sample length. Except for notational differences, these two expressions are identical.

Third Harmonic Generation

The third harmonic of an initially sinusoidal ultrasonic wave is built up by two processes: First is a three-phonon process in which the fundamental phonon (q_o,ω_o) and the second harmonic phonon (q_s,ω_s) annihilate to create the third harmonic phonon (q_t,ω_t), where $\omega_t = \omega_s + \omega_o = 3\omega_o$; and second is a four-phonon process in which three annihilating fundamental phonons (q_o,ω_o) create the third harmonic phonon (q_t,ω_t). We shall consider here only three-phonon processes which will give the significant terms found in the third harmonic amplitude. The four-phonon processes are ignored in the following.

Generation of the third harmonic gradually increases with the increase of the generation of the second harmonic. The second harmonic concentration at a distance L_x from the end of the sample is given by Eq. 21. This relationship is used in Eq. 11, along with the expression $dN_t/dt = v\, dN_t/dx$ to obtain the concentration of the third harmonic in the form

$$dN_t = \frac{1}{4}\left(\frac{\pi G^2_{q_1 q_2 q_3}}{8\rho^3 v^8}\right)^2 \omega_o^3 \omega_s^2 \omega_t n_o^3 x^3 dx \qquad (23)$$

Applying the boundary condition $N_3 = 0$ at $x = 0$, we find that the third harmonic can be expressed as

$$A_t = 2A_s^2/A_o \tag{24}$$

which is in very good agreement with the formula[3] obtained from considering the harmonic generation as a nonlinear process.[15] To facilitate comparison, we repeat Eq. 1 of Ref. 3 with slight notational changes:

$$A_t = 2A_0^3 L_x^2 q_0^4 \left(\frac{C_{111}+3C_{11}}{8C_{11}}\right)^2 \left\{1 + \frac{16}{9q_0^2 L_x^2}\left[1 - \frac{C_{11}(\frac{1}{2}C_{1111} + 3C_{111} + \frac{3}{2}C_{11})}{(C_{111} + 3C_{11})^2}\right]^2\right\}^{1/2} \tag{24a}$$

Comparison of Eqs. 24 and 24a leads to the conclusion that our neglect of four-phonon processes has dropped terms corresponding to the small term involving fourth-order elastic constants. This term was found to be negligible in the experiments reported in Ref. 3.

IV. PARAMETRIC DOWN-CONVERSION OF TWO ULTRASONIC WAVES AND PARAMETRIC AMPLIFICATION OF AN ULTRASONIC WAVE THROUGH ITS NONLINEAR INTERACTION WITH ANOTHER ULTRASONIC WAVE

The parametric down-conversion mixing process is observed as the generation of an ultrasonic wave of frequency ω_3 by two ultrasonic waves ω_1 and ω_2 such that $\omega_3 = \omega_1 + \omega_2$. This process can be described as a process in which a phonon $(\vec{q}_1,\omega_1)$ is annihilated, and phonons $(\vec{q}_2,\omega_2)$ and $(\vec{q}_3,\omega_3)$ are created. The process involving the annihilation of the phonon $(\vec{q}_1,\omega_1)$ and the creation of two new phonons is suggested in the Hamiltonian density (Eq. 3) by terms containing $\hat{a}_q\, \hat{a}^*_{q'}\, \hat{a}^*_{q''}$. Although spontaneous annihilation of a phonon has a very low probability of occurrence, the disintegration can be stimulated by the presence of one of the two components resulting from the annihilation.

Let us assume that the annihilation of the phonon $(\vec{q}_1,\omega_1)$ is stimulated by the presence of the phonon $(\vec{q}_2,\omega_2)$. We assume that there are N_1 phonons $(\vec{q}_1,\omega_1)$ and N_2 phonons $(\vec{q}_2,\omega_2)$ in the volume of normalization V under consideration. The amplitude of the transition from the initial state $|N_1,N_2,0>$ to the final state $|N_1-1,N_2+1,1>$ is given also in this case by Eq. 4, provided that N_1 and N_2 are much larger than unity. Repeating the procedure described in the previous section, one can again derive Eq. 11. This means that parametric down-conversion is described by the same formulae as the parametric up-conversion; however the down-conversion is accompanied by the effect of the amplification of the stimulating wave. The amplification of the stimulating wave results from the fact that the phonons $(\vec{q}_2,\omega_2)$, created from the disintegration of the phonons $(\vec{q}_1,\omega_1)$, contribute to the stimulating wave.

Let us now calculate the effect of the amplification, and simultaneously take into account the attenuation of the stimulating wave. We define the attenuation coefficient of an ultrasonic wave as

$$\alpha' = -\frac{1}{2N}\frac{dN}{dt} = -\frac{1}{2N}\frac{dN}{dx}v = \alpha v \ , \tag{25}$$

where α', the temporal attenuation coefficient, expresses the decrease of amplitude per unit of time, and α expresses the decrease per unit of length. Using this definition we can modify Eq. 11 to include attenuation:

$$\frac{dN_2}{dt} = \left(\frac{\hbar G^2 q_1 q_2 q_3}{8\rho^3}\frac{\omega_1\omega_2\omega_3}{v_1^2 v_2^2 v_3^3}L_x N_1 - 2\alpha_2'\right)N_2 \tag{26}$$

Assuming that $N_2 = 0$ at $t = 0$, the energy density of the stimulating wave at time $t = L_x/v_2$ is

$$p_2(L_x) = p_2(0)\exp\left[\frac{G^2 q_1 q_2 q_3 \omega_2 \omega_3}{8\rho^3 v_1^2 v_2^3 v_3^3} L_x^2 p_1 - 2\alpha_2 l_x\right] \tag{27}$$

where L_x is the length of the sample in the direction of the wave vector $\vec{q}_3 = \vec{q}_1 - \vec{q}_2$.

Influence of Attenuation on Nonlinear Interactions of Ultrasonic Waves

We have tacitly assumed that the attenuation of the interacting waves is zero in all previous sections except for the section on parametric down-conversion. This, however, never is completely true, and therefore this section will be devoted to discussion of the possible effect of ultrasonic attenuation on nonlinear interactions of ultrasonic waves.

As before, the total transition probability rate (Eq. 11) is equal to the total number of transitions per unit of time; i.e., it expresses the average number of phonons $(\vec{q}_3,\omega_3)$ created in the volume V_i per unit of time. With the help of Eq. 25 and Eq. 11 we can write for the concentration of phonons $(\vec{q}_3,\omega_3)$.

$$\frac{dN_3}{dt} = \frac{\hbar G^2 q_1 q_2 q_3}{8\rho^3} \frac{\omega_1 \omega_2 \omega_3}{v_1^2 v_2^2 v_3^3} L_x N_1 N_2 - 2\alpha_3' N_3 \tag{28}$$

If we assume that $N_1 = N_{01} e^{-2\alpha_1' t}$ and $N_2 = N_{02} e^{-2\alpha_2' t}$, when N_{01} and N_{02} are the concentrations of phonons at time $t = 0$, Eq. 28 has a solution of the form

$$N_3 = \frac{\hbar G^2 q_1 q_2 q_3}{8\rho^3} \frac{\omega_1\omega_2\omega_3}{v_1^2 v_2^2 v_3^3} L_x N_{01} N_{02} \left(\frac{e^{-2(\alpha_1'+\alpha_2')t} - e^{-2\alpha_3' t}}{2(\alpha_3'-\alpha_1'-\alpha_2')} \right) \tag{29}$$

Expanding the exponential functions and keeping only the linear terms, one has

$$N_3 = \frac{\hbar G^2 q_1 q_2 q_3}{8\rho^3 v_1^2 v_2^2 v_3^3} \omega_1\omega_2\omega_3 N_{01} N_{02} L_x [1-(\alpha_1'+\alpha_2'+\alpha_3')t]t \tag{30}$$

which is valid for small attenuation and short times t. From this, one sees that attenuation can be neglected, and Eq. 30 reduces to Eq. 19, when $(\alpha_1' + \alpha_2' + \alpha_3')\ t = (\alpha_1 + \alpha_2 + \alpha_3)\ \frac{L_x}{v} << 1$. In materials with a low value of attenuation, the attenuation coefficient often is expressed by $\alpha = A\ \omega^2$, where A is a constant of the order of magnitude 10^{-20} to 10^{-17} cm^{-1} sec^2. Using this condition, the attenuation is negligible if $\omega_1^2 + \omega_2^2 + \omega_3^2 << \frac{v}{AL_x}$. This condition usually is very well fulfilled when noncollinear interactions at frequencies between 10 and 100 MHz are investigated. Therefore, we shall go into greater detail only on collinear interactions.

Collinear interactions. Since the power of the ultrasonic wave can be written $P_i = \hbar\omega_i N_i L_y L_z v_i$, we can use Eq. 29 to write

$$P_3 = \frac{G^2 q_1 q_2 q_3 \omega_3^2}{8\rho^3 v_1^3 v_2^3 v_3^2} \frac{L_x}{L_y L_z} P_{01} P_{02} \left(\frac{e^{-2(\alpha_1'+\alpha_2')t} - e^{-2\alpha_3' t}}{2(\alpha_3'-\alpha_1'-\alpha_2')} \right) \tag{31}$$

Here L_x is interpreted to mean the effective interaction length, while t is the effective interaction time. Although this expression is limited to collinear interactions, it nevertheless is quite general in that it is valid for

describing the interaction of ultrasonic waves of different polarization modes.

If the interacting waves are of the same polarization mode we can again put $v_1 = v_2 = v_3 = v$ and write

$$P_3 = \frac{G^2_{q_1q_2q_3}\omega_3^2}{8\rho^3 v^9 L_y L_z} L_x^2 P_{01} P_{02} \left[\frac{e^{-2(\bar{\alpha}_1+\bar{\alpha}_2)} - e^{-2\bar{\alpha}_3}}{2(\bar{\alpha}_3-\bar{\alpha}_1-\bar{\alpha}_2)} \right] \tag{32}$$

where $\bar{\alpha}_n = \alpha_n L_x$ is the total attenuation of each wave over the sample length L_x. From this, the amplitude at the end of a sample of length L_x is found to be

$$A_3 = \frac{G_{q_1q_2q_3}}{4\rho v^2} q_1 q_2 A_{01} A_{02} L_x \left[\frac{e^{-2(\bar{\alpha}_1+\bar{\alpha}_2)} - e^{-2\bar{\alpha}_3}}{2(\bar{\alpha}_3-\bar{\alpha}_1-\bar{\alpha}_2)} \right]^{1/2} \tag{33}$$

Stabilization Distance

At a certain distance of propagation in the sample, the harmonic growth will be equal to the attenuation, with the result that a stabilization of the waveform will occur. This stabilization distance L_{max} can be calculated from Eq. 32 by taking the derivative and setting it equal to zero. For a sufficiently long sample the stabilization distance is

$$L_{max} = vt_{max} = \frac{\ell n(\alpha_1 + \alpha_2) - \ell n\, \alpha_3}{2(\alpha_1 + \alpha_2 - \alpha_3)} . \tag{34}$$

This is the distance at which the ultrasonic wave q_3 resulting from the nonlinear interaction has its maximum value.

Comparing this equation with that published in Ref. 6, one finds a difference of a factor of two. The origin of this difference is not known at present.

Second Harmonic Generation

Assuming that $A_{01} = A_{02} = A_0/\sqrt{2}$, the case of second harmonic generation by an originally sinusoidal ultrasonic wave of amplitude A_0 can be calculated. From Eq. 33 we find

$$A_s = \frac{G_{q_1 q_2 q_3}}{8\rho v^2} q_o^2 A_o^2 L_x \left(\frac{e^{-4\bar{\alpha}_o} - e^{-2\bar{\alpha}_s}}{2\bar{\alpha}_s - 4\bar{\alpha}_o} \right) \tag{35}$$

where $\bar{\alpha}_o$ and $\bar{\alpha}_s$ denote total attenuation of the primary wave and the second harmonic, respectively.

V. CONCLUDING REMARKS

We have discussed in some detail the nonlinear effects arising from the interaction of two ultrasonic waves. As has been mentioned, there is good agreement between our results and the results in Refs. 1, 2, 3 and 15, if one compares the particular limiting cases of our general treatment with the results in these papers. This agreement is a valuable result because it shows that in the correspondence limit the quantum mechanical description of harmonic generation gives the same results as classical calculations for both the second harmonic amplitude and the third harmonic amplitude. This emphasizes the point that nonlinear interactions are a unique and powerful tool for the measurement of the nonlinear properties of materials.

Finally, we shall discuss the limiting assumption concerning the power of the generated wave. In discussing the nonlinear ultrasonic interactions

we have assumed that the initial state of the created phonons is empty. This means that only the beginning of the generation process has been considered. This is exactly the situation described in a previous paper based on classical calculations.[1] But in the present situation this does not put an essential limitation on our considerations. If the initial state of the created phonons were not initially empty, the "back scattering" should be taken into account. This situation can be described symbolically by

$$\left|\langle N_1-1, N_2-1, N_3+1|\hat{H}_{int}|N_1, N_2, N_3\rangle\right|^2 - \left|\langle N_1+1, N_2+1, N_3-1|\hat{H}_{int}|N_1, N_2, N_3\rangle\right|^2 \tag{36}$$

$$\simeq N_1N_2 - (N_1+N_2)N_3$$

The situation described in our discussion is obtained if $N_1 = N_2 >> N_3$. It can be shown that the correction for "back scattering" is about 2% when the power of the generated wave is about 1% of the primary waves. In most practical cases the power of the generated wave is much lower than 1% of the power of the primary wave. Therefore, the equations we have derived are adequate to describe most experimental situations.

Acknowledgment

Research supported in part by the International Research and Exchanges Board and in part by the Office of Naval Research.

[a]Present address: College of Advanced Transport Engineering, Department of Physics, 01088 Zilina, Czechoslovakia.

1. M. A. Breazeale and J. Ford, J. Appl. Phys. 36, 3486 (1965)

2. J. A. Bains, Jr. and M. A. Breazeale, J. Acoust. Soc. Am. 57, 745 (1975).

3. R. D. Peters and M. A. Breazeale, Appl. Phys. Letters 12, 106 (1968).

4. E. M. Conwell and A. K. Ganguly, Phys. Rev. B 4, 2535 (1971).

5. H. N. Spector, Phys. Rev. B 7, 1420 (1973).

6. N. R. Valitova and K. V. Goncharov, Fiz. Tverd. Tela 12, 3089 (1970) [Sov. Phys.-Solid State 12, 2499 (1971).

7. L. H. Taylor and F. R. Rollins, Jr., Phys. Rev. 136, A591 (1964).

8. F. R. Rollins, Jr., L. H. Taylor, and P. H. Todd, Jr., Phys. Rev. 136, A597 (1964).

9. Yosio Hiki and Kiichiro Mukai, J. Phys. Soc. Japan 34, 454 (1973).

10. R. W. Dunham and B. H. Huntington, Phys. Rev. B 2, 1098 (1970).

11. A. C. Holt and J. Ford, J. Appl. Phys. 40, 142 (1969).

12. I. L. Bajak, Wave Electronics 3, 51-68 (1977).

13. A. S. Davydov, Quantum Mechanics (NeoPress, Ann Arbor, Mich., 1948), p. 554.

14. The interaction Hamiltonian density, Eq. (5), has been obtained on the basis of Eq. (2). It cannot be compared mechanically with the Hamiltonian density obtained, for example, by Hiki and Mukai (Ref. 9). Hiki and Mukai derived their formula from an expansion of the free energy density by considering only the elastic potential energy. In general, the expansion of the free energy density has the form

$$\phi = \phi_o + \frac{1}{2} C^E_{ijk\ell} S_{ij} S_{k\ell} + \frac{1}{3!} A^E_{ijk\ell mn} S_{ij} S_{k\ell} S_{mn} + \frac{1}{2} \epsilon^S_{ij} E_i E_j$$

$$+ \frac{1}{2} D_{ijk} E_i S_{jk} + \frac{1}{3!} G_{ijk\ell} E_i E_j S_{k\ell} + \cdots$$

where the E_i are the components of a macroscopic applied electric field, and the other terms account for interaction between the electric field and the displacements. A coupled-mode description of these interactions can be found in the book by Donald F. Nelson, Electric, Optic, and Acoustic Interactions in Dielectrics (Wiley, New York, 1979), p. 446. The constants $C_{ijk\ell}$ in our relation (2) are stiffened, and also there is a contribution to the stiffening by the terms $\partial C_{ijk\ell}/\partial S_{mn}$. Taking into account the contribution of the stiffening we can put

$$\partial C_{ijk\ell}/\partial S_{mn} = A_{ijk\ell mn}/3 \ ,$$

where the $A_{ijk\ell mn}$ are the third-order elastic moduli stiffened by the presence of an ultrasonic wave. The C_{mnpqrs} of Hike and Mukai describe the undisturbed medium, and are not stiffened in this way.

15. M. J. P. Musgrave, Crystal Acoustics (Holden-Day, San Francisco, 1970), p. 145.

16. R. N. Thurston and M. J. Shapiro, J. Acoust. Soc. Am. 41, 1112 (1967).

REPORTS DISTRIBUTION LIST FOR ONR PHYSICS PROGRAM OFFICE
UNCLASSIFIED CONTRACTS

Director Defense Advanced Research Projects Agency Attn: Technical Library 1400 Wilson Blvd. Arlington, Virginia 22209	3 copies
Office of Naval Research Physics Program Office (Code 421) 800 North Quincy Street Arlington, Virginia 22217	3 copies
Office of Naval Research Assistant Chief for Technology (Code 200) 800 North Quincy Street Arlington, Virginia 22217	1 copy
Naval Research Laboratory Department of the Navy Attn: Technical Library Washington, DC 20375	3 copies
Office of the Director of Defense Research and Engineering Information Office Library Branch The Pentagon Washington, DC 20301	3 copies
U.S. Army Research Office Box 12211 Research Triangle Park North Carolina 27709	2 copies
Defense Documentation Center Cameron Station (TC) Alexandria, Virginia 22314	12 copies
Director, National Bureau of Standards Attn: Technical Library Washington, DC 20234	1 copy
Commanding Officer Office of Naval Research Branch Office 536 South Clark Street Chicago, Illinois 60605	3 copies

Commanding Officer Office of Naval Research Branch Office 1030 East Green Street Pasadena, California 91101	3 copies
San Francisco Area Office Office of Naval Research One Hallidie Plaza Suite 601 San Francisco, California 94102	3 copies
Commanding Officer Office of Naval Research Branch Office 666 Summer Street Boston, Massachusetts 02210	3 copies
New York Area Office Office of Naval Research 715 Broadway, 5th Floor New York, New York 10003	1 copy
Director U.S. Army Engineering Research and Development Laboratories Attn: Technical Documents Center Fort Belvoir, Virginia 22060	1 copy
ODDR&E Advisory Group on Electron Devices 201 Varick Street New York, New York 10014	3 copies
Air Force Office of Scientific Research Department of the Air Force Bolling AFB, D.C. 22209	1 copy
Air Force Weapons Laboratory Technical Library Kirtland Air Force Base Albuquerque, New Mexico 87117	1 copy
Air Force Avionics Laboratory Air Force Systems Command Technical Library Wright-Patterson Air Force Base Dayton, Ohio 45433	1 copy
Lawrence Livermore Laboratory Attn: Dr. W. F. Krupke University of California P.O. Box 808 Livermore, California 94550	1 copy

Harry Diamond Laboratories — 1 copy
Technical Library
2800 Powder Mill Road
Adelphi, Maryland 20783

Naval Air Development Center — 1 copy
Attn: Technical Library
Johnsville
Warminster, Pennsylvania 18974

Naval Weapons Center — 1 copy
Technical Library (Code 753)
China Lake, California 93555

Naval Training Equipment Center — 1 copy
Technical Library
Orlando, Florida 32813

Naval Underwater Systems Center — 1 copy
Technical Library
New London, Connecticut 06320

Commandant of the Marine Corps — 1 copy
Scientific Advisor (Code RD-1)
Washington, DC 20380

Naval Ordnance Station — 1 copy
Technical Library
Indian Head, Maryland 20640

Naval Postgraduate School — 1 copy
Technical Library (Code 0212)
Monterey, California 93940

Naval Missile Center — 1 copy
Technical Library (Code 5632.2)
Point Mugu, California 93010

Naval Ordnance Station — 1 copy
Technical Library
Louisville, Kentucky 40214

Commanding Officer — 1 copy
Naval Ocean Research & Development Activity
Technical Library
NSTL Station, Mississippi 39529

Naval Explosive Ordnance Disposal Facility — 1 copy
Technical Library
Indian Head, Maryland 20640

Naval Ocean Systems Center — 1 copy
Technical Library
San Diego, California 92152

Naval Surface Weapons Center — 1 copy
Technical Library
Dahlgren, Virginia 22448

Naval Surface Weapons Center (White Oak) — 1 copy
Technical Library
Silver Springs, Maryland 20910

Naval Ship Research and Development Center — 1 copy
Central Library (Code L42 and L43)
Bethesda, Maryland 20084

Naval Avionics Facility — 1 copy
Technical Library
Indianapolis, Indiana 46218

Dr. Werner G. Neubauer — 1 copy
Code 8130
Physical Acoustics Branch
Naval Research Laboratory
Washington, DC 20375

Dr. Bill D. Cook — 1 copy
Dept. of Mechanical Engineering
University of Houston
Houston, Texas 77004

Dr. Floyd Dunn — 1 copy
Biophysical Research Laboratory
University of Illinois
Urbana, Illinois 61801

Dr. E. F. Carome — 1 copy
Department of Physics
John Carroll University
University Heights
Cleveland, Ohio 44017

Albert Goldstein, Ph.D. — 1 copy
Chief, Division of Medical Physics
Henry Ford Hospital
2799 West Grand Boulevard
Detroit, Michigan 48202


DATE
ILME